2007

APPROACHES TO MOLECULAR IMPRINTING ON POLYSILOXANE SCAFFOLDS

Michael Edward Brown
University of Kentucky, gyrus9@gmail.com

ABSTRACT OF THESIS

APPROACHES TO MOLECULAR IMPRINTING ON POLYSILOXANE SCAFFOLDS

Molecular imprinting, a common method used in separations and chromatography to isolate specific molecules via surface binding, has been adapted for applications in biomaterials and related sciences. The objective of this study was to determine the effectiveness of different approaches to molecular imprinting by testing for preferential binding of protein on polysiloxane scaffold surfaces. To test preferential rebinding, the scaffolds were exposed to a mixture of the template protein and a competitor protein with similar size but different chemistry. Lysozyme-imprinted polymers rebound 8.13 ± 0.99% of lysozyme without any competition and 5.1 ± 0.3% of the protein during competition. Lysozyme C peptide was imprinted into polysiloxane scaffolds to investigate the "epitope approach" to molecular imprinting. Without competition, 8.95 ± 11.53% of the lysozyme preferentially bound to the scaffolds, while under competition 1.85 ± 9.47% bound to the scaffolds. Lastly, bone morphogenetic protein 2 (BMP-2) was imprinted into the polymer scaffolds. Results revealed that BMP-2 imprinted scaffolds bound 10.09 ± 6.625% under noncompetitive conditions and a very small 0.65 ± 4.55% during competition. Trends of preferential binding via peptide imprinting and BMP-2 imprinting can be seen, and show promise in future tissue engineering material applications and biomaterial compatibility.

KEYWORDS: Molecular imprinting, epitope approach, polysiloxane, sol-gel processing, preferential binding

Multimedia Elements Used: TIFF (.tif)

Michael Edward Brown
2 August 2007

APPROACHES TO MOLECULAR IMPRINTING ON POLYSILOXANE SCAFFOLDS

By

Michael Edward Brown

David A. Puleo, Ph.D.
Director of Thesis

Abhijit Patwardhan, Ph.D.
Director of Graduate Studies

2 August, 2007

RULES FOR THE USE OF THESES

Unpublished theses submitted for the Master's degree and deposited in the University of Kentucky Library are as a rule open for inspection, but are to be used only with due regard to the rights of the authors. Bibliographical references may be noted, but quotations or summaries of parts may be published only with the permission of the author, and with the usual scholarly acknowledgments.

Extensive copying or publication of the thesis in whole or in part also requires the consent of the Dean of the Graduate School of the University of Kentucky.

A library that borrows this thesis for use by its patrons is expected to secure the signature of each user.

APPROACHES TO MOLECULAR IMPRINTING ON POLYSILOXANE SCAFFOLDS

Michael Edward Brown

The Graduate School
University of Kentucky
2007

APPROACHES TO MOLECULAR IMPRINTING ON POLYSILOXANE SCAFFOLDS

THESIS

A thesis submitted in partial fulfillment of the requirements
for the degree of Master of Science in Biomedical Engineering
in The Graduate School at the University of Kentucky

By

Michael Edward Brown

Lexington, KY

Director: Dr. David A. Puleo, Professor of Biomedical Engineering

Lexington, KY

2007

Acknowledgments

I would like to thank my advisor Dr. David Puleo for all of his patience and guidance throughout the entire process of constructing this thesis. It is not an understatement when I say that without his extraordinary drive and support, I wouldn't have made it this far in graduate school. I thank him for giving me the opportunity to study at the Center for Biomedical Engineering and helping me in becoming an inquisitive and insightful engineer. I would also like to thank my committee members Dr. Marnie Saunders and Dr. Betty Sisken for forcing me to think outside the box and for being a wonderful part of my transition into the next phase of my career.

I would like to thank my good friend and coworker Randy Hilliard for keeping me sane during all the rough times and for always being there when I needed clarity, intuition, and a good laugh. I want to thank Joey and Shaun for their support and wisdom in writing this thesis and for all the times when I needed to stop writing have fun. I would also like to thank all of my peers and professors at the Center for Biomedical Engineering for making a great working environment, and all of the people I've come in contact with here during my stay in Lexington.

I also want to acknowledge all my great friends from back home in Tucson, Arizona. In case they were wondering why I've been anti-social, let this be a good enough reason. I am grateful for my mom and dad for not only pushing me to great heights, but for always believing in me and never letting me down when I needed encouragement. I thank especially Betsy Chatham for being there when I needed her most and for being extraordinarily selfless and caring at all times.

Table of Contents

List of Tables

List of Figures

1. Introduction

The advancement in treatment of human bone damage has reached an astonishing level. In understanding the mechanisms of bone healing and formation, medicine has climbed to a position where most bone dysfunctions and injuries can be reasonably remedied. For cases such as a simple fracture, bone is stabilized and allowed to heal itself. Extensive bone damage resulting from comminuted and compound fractures are repaired using devices geared toward internal methods, such as pins, that hold bone together or implants that replace the tissue. Many bone biomaterials, such as metal, ceramic, polymer, and composite implants, now play an integral part in repairing bone and cartilage function [1]. Despite these advances, there is still a need for a more efficient method of bone repair that circumvents the problems created by conventional procedures, such as bio-incompatibility, premature failure, harmful invasive surgery, and costs.

Tissue engineering, a recently developed field of science, brings a new hope for not only tissue repair but regeneration [2]. The concept involves growing new and healthy tissue when normally the body could not do so otherwise using a sophisticated strategy with biomolecules, cells, and a scaffold matrix. The combination of biology and engineering has already led to incredible breakthroughs in clinical studies including skin and cartilage tissue replacement [3]. Among the various methods of protein immobilization, molecularly imprinted polymers (MIPs) have been recently investigated and used for many applications. Polymers such as polyacrylics and silicas are polymerized with biomolecules that when removed, form an imprint mimicking its identical shape and chemical arrangement [4]. The key ability of the MIP is to rebind what it has imprinted when it is exposed to a biological system.

In the past, MIPs have been used for imprinting simple biomolecules, such as sugars, steroids, certain drugs and pesticides [5]. Not until recently have larger biomolecules, such as proteins been used with MIPs for many applications such as molecular recognition assays [4, 6, 7]. Among countless other purposes,

cells use protein as extracellular cues to start attachment, differentiation, communication, and intracellular processes. In this light, proteins can be selectively adhered to MIPs for the purpose of controlled cellular behavior, from cell adhesion to eventual matrix construction and tissue growth.

The aim of this study, therefore, was two-fold. The first was to investigate the potential for molecular imprinting using two types of molecules, one being the protein and the other a peptide found on its surface. Protein imprinting has been seen in studies, but whether or not imprinting with just a small peptide section of it produces the same binding preference has not been studied in great detail. Secondly, bone morphogenetic protein 2 (BMP-2), a protein found to be an important growth factor in osteogenesis, was investigated for its potential in preferential binding to polysiloxanes MIPs for controlled cellular behavior *in vitro*.

2. Background and Significance

2.1. Current Approaches to Meeting the Need for Bone Repair

A major interest among the medical field is the need for optimization of bone damage repair. In most cases of bone damage therapy, the degree of treatment depends on the severity of the injury or defect. For a simple injury such as a linear fracture in a bone, a closed reduction treatment is applied [8-10]. In this instance, the fracture is reduced by natural bone healing through external stabilization techniques, such as a plaster cast [11, 12]. As long as the bone ends are united and micromotion is avoided, healing of the fracture will result in a minimal loss of function. For a complex bone injury that produces segmented bone, bone fragments, or large voids in the tissue, a more intricate approach is necessary for replacing normal function. Open reduction involves reducing fractures through the use of careful surgery. In a case where the bone has been shattered, the affected area is cut open and nails are usually used in conjunction with metal rods and plates to piece the tissue back into its proper place so that the bone can be healed in the correct position [12, 13] (Figure 1). Displaced fractures have a high incidence of avascular necrosis, pseudoarthrosis (a fake joint), and refracture [14]. In any case, mild fractures when treated properly and allowed a period of decreased activity, will result in rapid healing, and return to full activity, whereas more severe fractures will require more intervention and a longer recovery period [14].

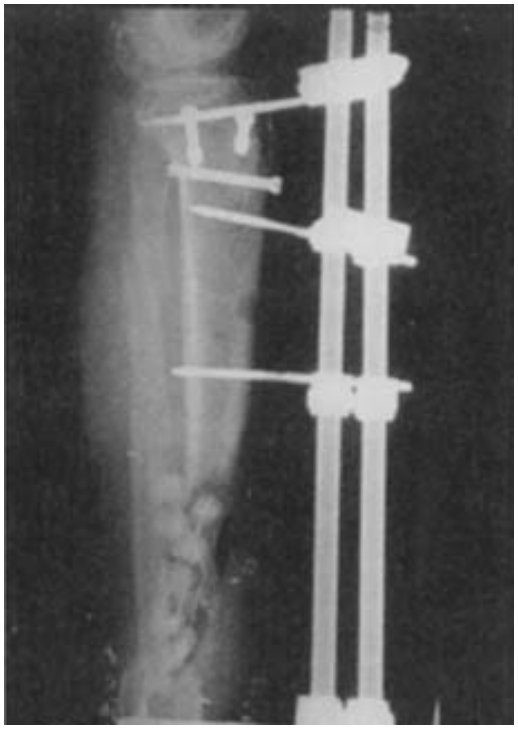

Figure 1. The use of an Ilizarov frame for bone transport in an infected nonunion of an open tibia fracture [11].

Oftentimes, injury or disease can cause voids in the bone beyond a certain “critical size”, such that complete calcification of the wound will not occur [15]. In a mathematical model developed by J.S. Arnold, the range for a reasonable estimate of the critical size defect is from 0.4 cm up to 1.5 cm for animals such as rats, rabbits, dogs, pigs, and monkeys [15]. These voids can come from implant failure [16], serious bone trauma, and disease like osteoporosis and cancer where the structure of the bone becomes increasingly susceptible to damage [17, 18]. New approaches involving bone grafting and tissue engineering are now under investigation for solving large void volume problems. These new techniques have the ability to grow new bone tissue using the strategic involvement of biology and materials engineering [19]. Grafting of a patient’s own bone is ideal from the perspective of rejection and osteogenic potential while producing the best clinical results [20]. Ideally, tissue engineering will enable bone growth to bridge the gap and replace the large void that was once unfixable with natural tissue [21].

Tissue engineering techniques are quite new and still under rigorous study. The reason why these methods of bone healing are so sought after is their efficiency of restoring proper bone tissue and function. In fact, such methods may be able to replace bone tissue in places where before it has been impossible.

2.2. Wound Healing in Bone

In order to optimize the performance of a bone biomaterial, it is important to understand the physiology behind natural bone tissue. The most successful implant or bone graft is the one that best utilizes the natural properties and components of bone [22]. The process in which bone heals and regenerates is, therefore, crucial in the development of a material that helps in replacing bone tissue function [23].

The wound healing process is initiated immediately after a fracture has occurred or a defect is created in the bone tissue [24]. The first course of action is exudation of fluid and protein to the injured site [10]. Neutrophils and macrophages begin to clean up the wound by identifying small foreign objects and small fragments of bone. Platelets are concentrated at areas of damaged blood vessels to induce hemostasis and blood clotting. After a short time, the damaged tissue site becomes inflamed and induces chemical mediators such as proteases, cytokines, and growth factors [25]. Continual clotting creates a fracture hematoma where fibroblasts and macrophages are recruited [10]. Fibroblasts produce new collagen fibers and an aggregate of loose cells interspersed with new blood vessels (granulation tissue) while the macrophages engulf any harmful biomolecules [26, 27]. Concurrently, cells of the periosteum begin to replicate and differentiate, many of which have osteogenic potential. These cells migrate to the wound and transform into specialized cells, each playing a specific role in bone regeneration [10] (Figure 2). Dead bone fragments around the site are resorbed and dissolved by osteoclasts, while osteoblasts produce new trabeculae which eventually become spongy bone and later compact bone [28]. The differentiation of osteogenic cells into osteoblasts

is triggered by the abundance of many localized growth factors, such as fibroblast growth factor (FGF), prostaglandins, and transforming growth factor beta (TGF-β) [29, 30]. Released due to the wound healing response during inflammation, BMP-2, a member of the TGF-β family of growth factors, has been shown to repair and induce bone formation [30]. It is for this reason that BMP-2 is so widely studied in bone grafting and implant compatibility.

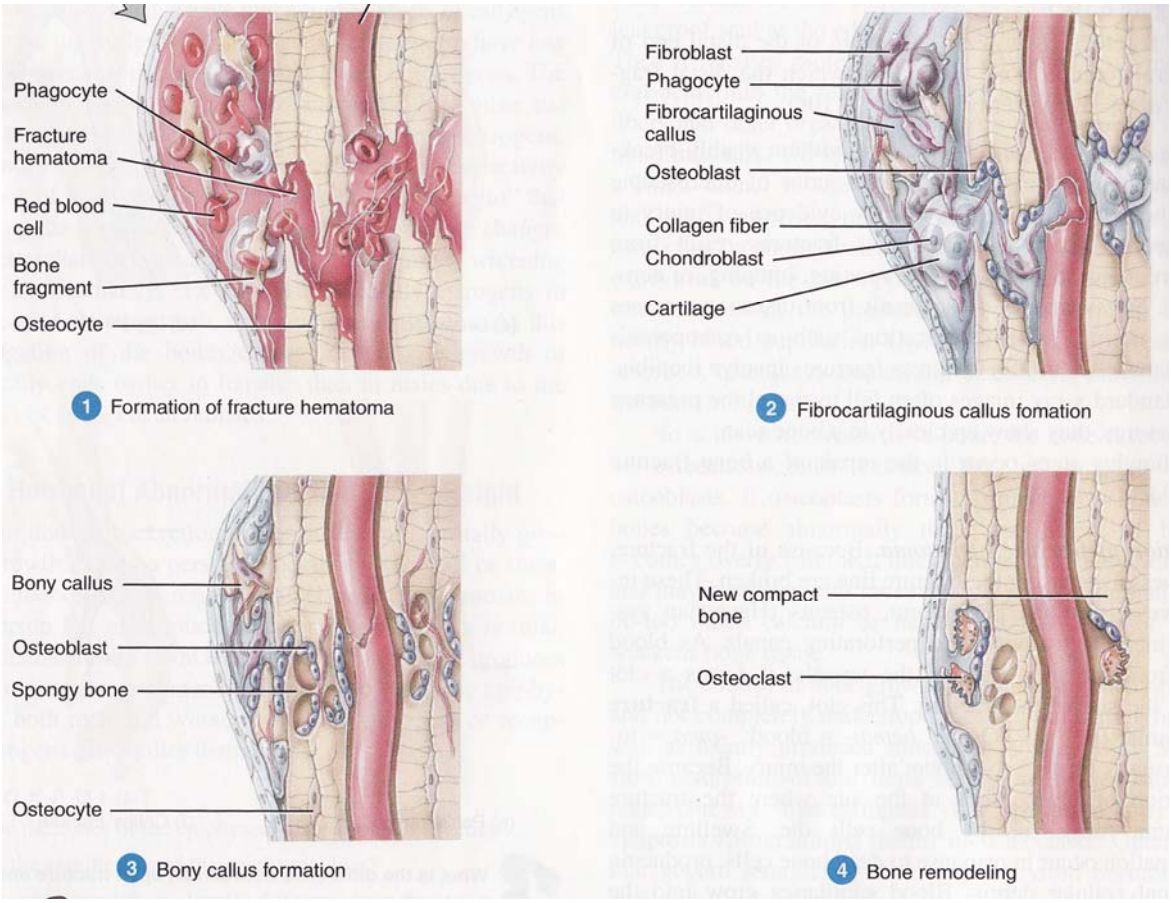

Figure 2. Steps of the bone healing process [10].

2.3. General Tissue Engineering Concepts

Tissue engineering is a widely studied approach for bodily tissue and organ replacement therapies. It involves growing or repairing the tissue in a host using a combination of components found in the natural physiological environment and a biomimetic material that is recognized by cells via chemical or

physical methods [31]. Tissue engineering is accomplished under the use of three main components: 1.) protein or other biomolecules that are specific in function, 2.) cells which are used in tissue regeneration, and 3.) an extracellular matrix which is mimicked by a porous scaffold [3, 32] (Figure 3). The type and amount of protein and biomolecules incorporated in the engineered scaffold, as well as the surface characteristics (i.e., chemistry and roughness) of the implant will have a profound influence on cell type migration and proliferation [33] . Since a biomaterial is considered a foreign object inside the body, certain proteins attached to the scaffold matrix may help in reducing an immune response [26]. Cells are a crucial element in tissue engineering because they begin the manufacture of tissue. Once a cell is able to safely attach, it begins producing growth factors that acts as a communicator for other cells to attach and migrate to the site [18]. Eventually, chemical mediators in the system begin to signal for the cells to differentiate into specific cell types that start producing the building blocks of new tissue. The scaffold used in tissue engineering techniques is of particular importance because it has several significant functions. For one, the scaffold may act as a temporary mechanical replacement for the original tissue such as in bone or cartilage [26]. Secondly, the porous nature of the scaffold allows cells to infiltrate into the pores and proliferate much like in native tissue [21]. Attachment and controlled activity of the cells can also be achieved with greater success by incorporating proteins and biomolecules into the scaffold's lattice structure [34]. In the case of a biodegradable bone scaffold matrix, structural function is slowly transferred to the new bone while the temporary biomaterial degrades away, thereby growing completely new permanent tissue without still having foreign material in the body [35]. These types of scaffolds are made from both natural (i.e., collagen, fibrin) and synthetic polymer (i.e., poly(lactic-co-glycolic acid)) materials [26].

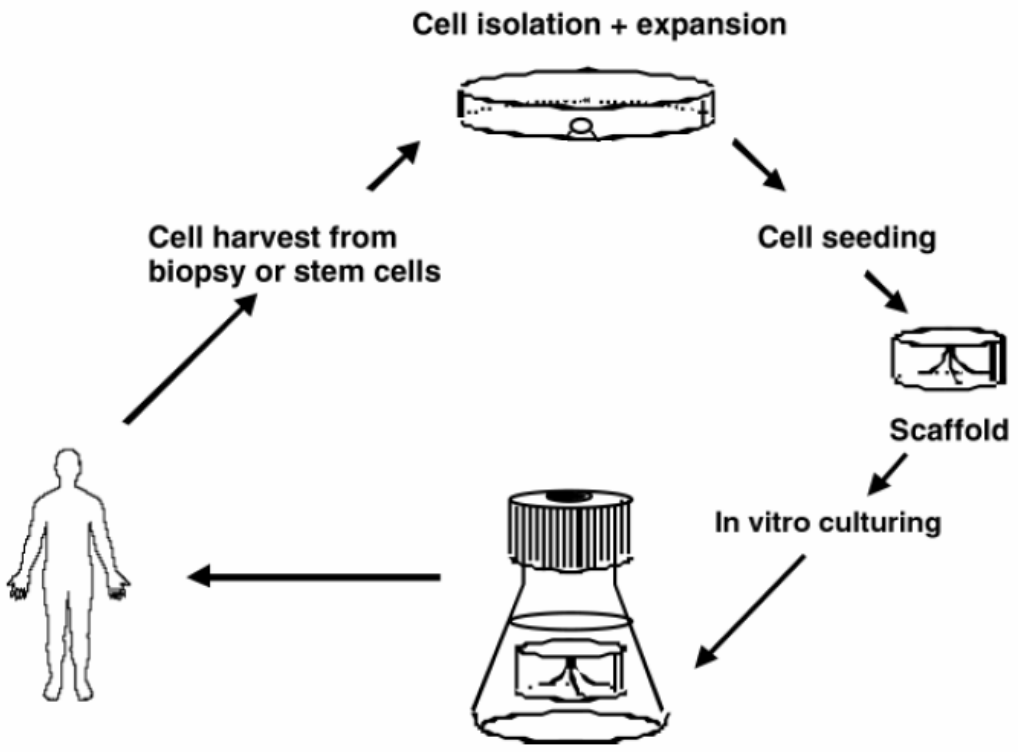

Figure 3. The basic concept of tissue engineering [3].

2.4. Basic Protein Characteristics

Proteins are of great importance for both tissue engineering efficiency and controlling overall cellular behavior. It has been shown that signaling proteins control the cellular behaviors associated with tissue formation. Understanding the underlying principles of proteins are crucial for an effective collaboration between a biomaterial and controlled cellular activity [36]. The very basic unit of a protein is the amino acid. A chain of amino acids in a particular sequence are what make up a polypeptide, or a protein's primary structure. As the peptide chain grows in length, the functional groups that make up the amino acids begin to interact with each other, bending and twisting the chain into what is known as the protein's secondary structure. Common forms of the secondary structure are the alpha helix and the beta sheet. Continual growth of the chain induces a larger number of intramolecular interactions where secondary structures are now greatly affected by each other. The result forms a tertiary

structure, which describes how the entire protein molecule coils into an overall three-dimensional shape. Quaternary structures may be attained with some but not all proteins by bonding and chemically interacting between different polypeptide chains in the molecules [10, 37].

Because of their chemical constitution, proteins have a tendency to bind to many surfaces. In most cases, when a material is exposed to the blood stream, many small proteins will instantly adhere to the surface non-specifically [23]. This adhesion is created by electrostatic forces and hydrophobic interactions from the chemistry of the protein and the surface chemistry of the biomaterial [38]. Specific adsorption occurs when the surface of a material binds protein using specialized spatial or chemical devices such as a cell receptor or extracellular matrix biomolecules. In such cases, molecular bonds like hydrogen bonding and ionic bonding are involved in the ligand-receptor complex [26].

As mentioned before, while non-specific adsorption relates to random protein placement, specific adhesion relates to selective placement, which is crucial because of the effects protein has at the cellular level. Figure 4 shows a schematic of the BMP-2 protein and receptor complex. When a particular protein is present in the vicinity of a cell, binding of the protein via a specific surface receptor will induce a cascade of events that will change the activity of the cell [39]. As previously discussed, BMP-2 is a member of the transforming growth factor family that plays an important role in bone healing. When bound to the surface receptor, the protein induces differentiation of resident mesenchymal cells into bone cells [40]. Similar to an enzyme binding a substrate, the BMP-2 receptor on the cell's surface will only recognize the specific shape and chemistry of BMP-2. Once binding of the protein occurs, a series of intracellular events takes place that result in the cell's maturation. The signaling cascade starts when BMP-2 contacts the BMP receptors. Phosphorylation of the receptor protein forms the transducing complex, which phosphorylates the Smad proteins (i.e. Smad-1, Smad-5, and Smad-8). Smad-1 and Smad-5 enter the nucleus of the mesenchymal cell after interacting with Smad-4 and initiate the BMP response genes. Smad-6 and Smad-7 inhibit phosphorylation of Smad-5, while

noggin and chordin, are BMP antagonists and prevent receptor binding [41] (Figure 5).

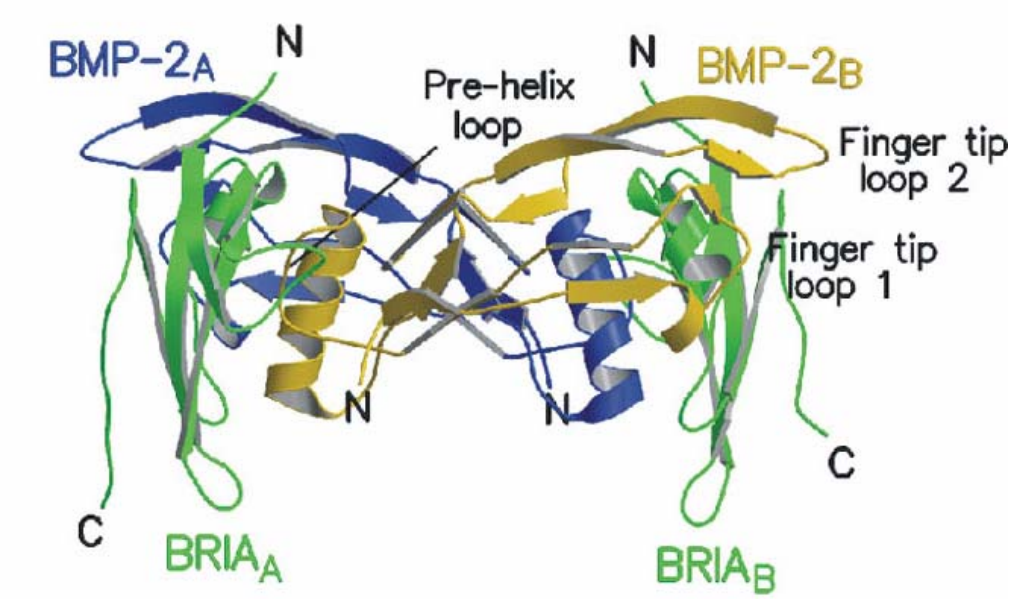

Figure 4. A diagram of bone morphogenetic protein 2 (BMP-2) bound to its cell receptor BMP receptor type IA (BRIA) [42].

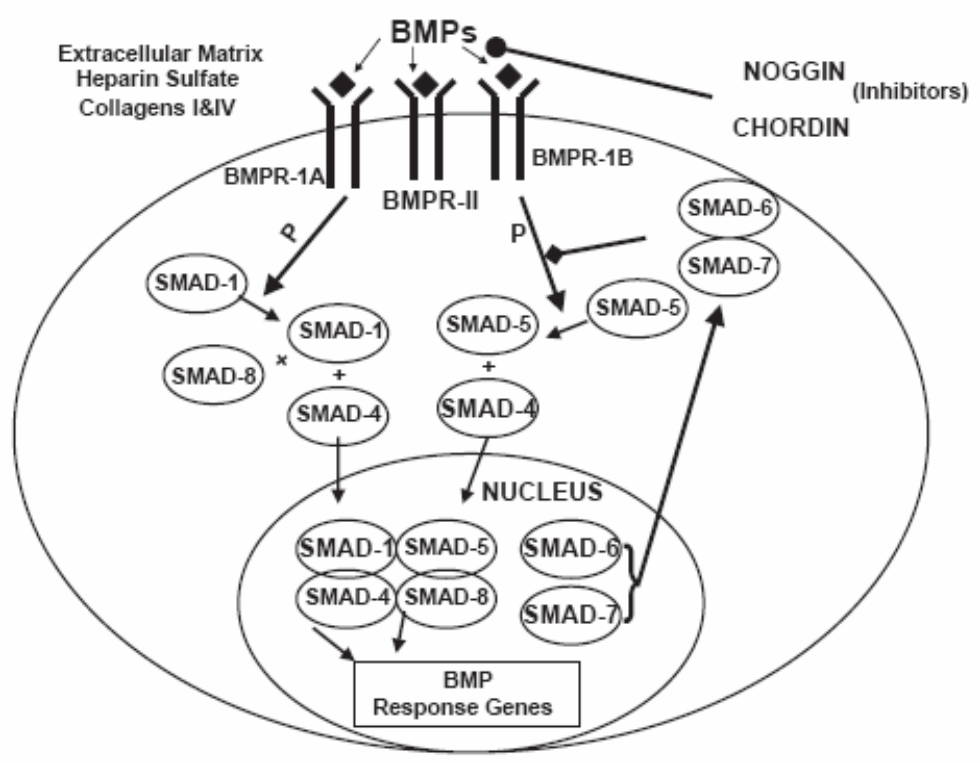

Figure 5. The BMP intracellular and signaling cascade [41].

2.5. Molecular Imprinting

As a way of creating a material with specific protein adsorption properties, molecular imprinting has been developed through years of study. The process involves the fabrication of a material with molecular structures initially embedded in the biomaterial. When the molecules on the surface are removed, they leave behind a crevice with the same physical shape. In addition, the same spatial orientation of complementary chemical groups that bound the molecule in the material is preserved. As a result, the same molecule (or 'template') used to make the imprint is able to specifically rebind even under environments that contain other competing molecules (or 'competitor') [6, 43, 44].

The most common molecularly imprinted materials are polymers due to their ability to chemically cross-link the template molecule. In general, these polymers, termed molecularly imprinted polymers (MIPs), are formed from: 1.) a cross-linking agent, 2.) a functional monomer, and 3.) the template molecule (Figure 6). The template molecule is mixed with the functional monomer so that chemical bonds between the two are formed. The cross-linking agent binds to the functional monomers upon polymerization, which embeds the template molecule in a polymer matrix. The molecules that are embedded on the surface when removed are the primary contributors to the imprints. Because the functional monomers are bound to the template in a specific position within the polymer, removal of the molecule will result in an imprint with both spatial and chemical preservation. Now, the structure of the polymer at this location is a mirror of the template molecule and is able to rebind that molecule preferentially over other competitor molecules that do not share the same physical and chemical structure [4, 43, 45].

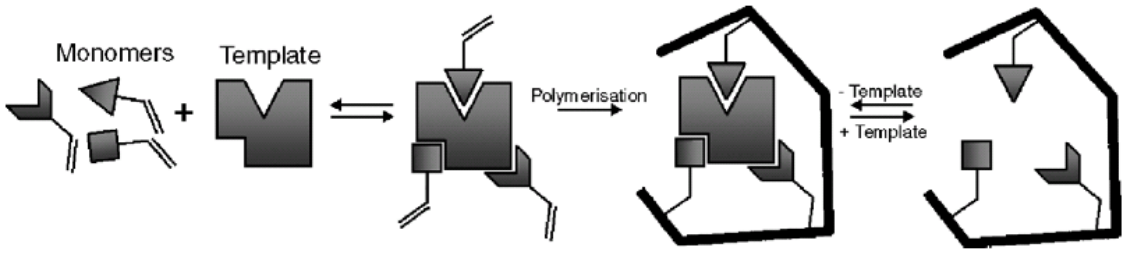

Figure 6. Schematic generalization of the molecular imprinting process [46].

In the early history of MIPs, small biomolecules, such as sugars, cholesterols, and certain drugs, were used as a template because of their simplicity and stability. Recently however, proteins have been the focal point of many MIP studies for uses in biomaterial compatibility, medical diagnostics, drug delivery, and tissue engineering [5]. The chemical structure of protein consisting of several functional groups allows many binding opportunities for a variety of functional monomers, provided the interaction is on the surface of the molecule. Polymerization of the protein is usually safe under tolerable conditions, and removal of the protein can be accomplished using a protease to digest the protein while keeping the functional monomers intact for rebinding. Unlike the simple template molecules used before it, however, protein as a template produces quite a few problems. Because proteins are large, sensitive, and unstable molecules, imprinting with these molecules can be very difficult [7]. Conditions such as pH, pressure, and temperature can have an influence on the protein's structure at the time of polymerization and create errors in the imprinting process. The protein's flexible structure also makes it difficult to achieve efficient and consistent binding results [4]. In other words, the physical shape of the protein may bend or stretch from other obstacles, such as biomolecules or movement of the surrounding fluid, creating a form unrecognizable to the rigid surface of the material. Many studies are currently underway to address these problems by developing newer methods of imprinting (i.e., [47, 48]). For instance, hydrogels are being studied in drug delivery applications for alterations in gel characteristics in response to factors such as pH, temperature, and ionic

strength of a solution. A gel that can modify its swelling behavior can in turn alter its ability to bind molecules.

While imprinting MIPs with protein is becoming a popular concept, a new approach to protein imprinting, called the epitope approach, is being explored [5] (Figure 7). The epitope approach is so named due to its similarity in concept of the antigen-antibody complex. When an antibody of the immune system binds a specific antigen, it does not need to recognize the presence of the entire molecule, but rather only a small portion of it. This small peptide sequence on the antigen, called the epitope, is the site where the antibody specifically binds and influences an immune response. Likewise, it may be possible to bind a large macromolecule such as a protein to a surface with only using a small peptide or 'epitope' section [5]. In a MIP, a peptide sequence on the surface of the protein is isolated and imprinted into the material. When the original protein is exposed to the imprint, the small peptide on its surface that was imprinted recognizes its spatial and chemical mimic in the polymer and binds. In this fashion, only a portion of the entire molecule is needed for preferential binding, which shows potential for optimization of protein immobilization. Figure 8 shows a schematic that illustrates a comparison between protein and peptide imprinting.

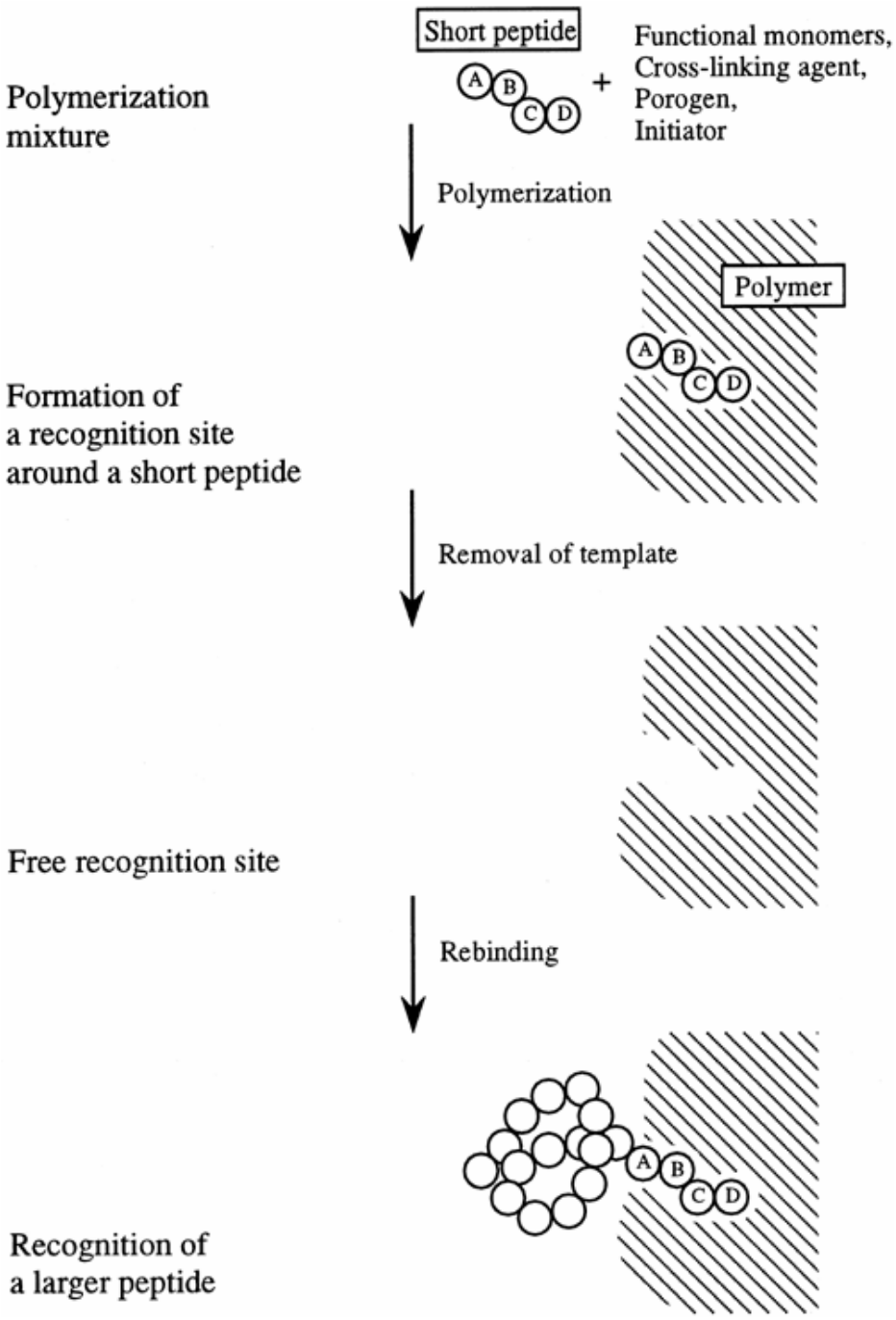

Figure 7. Schematic representation of the epitope approach [5].

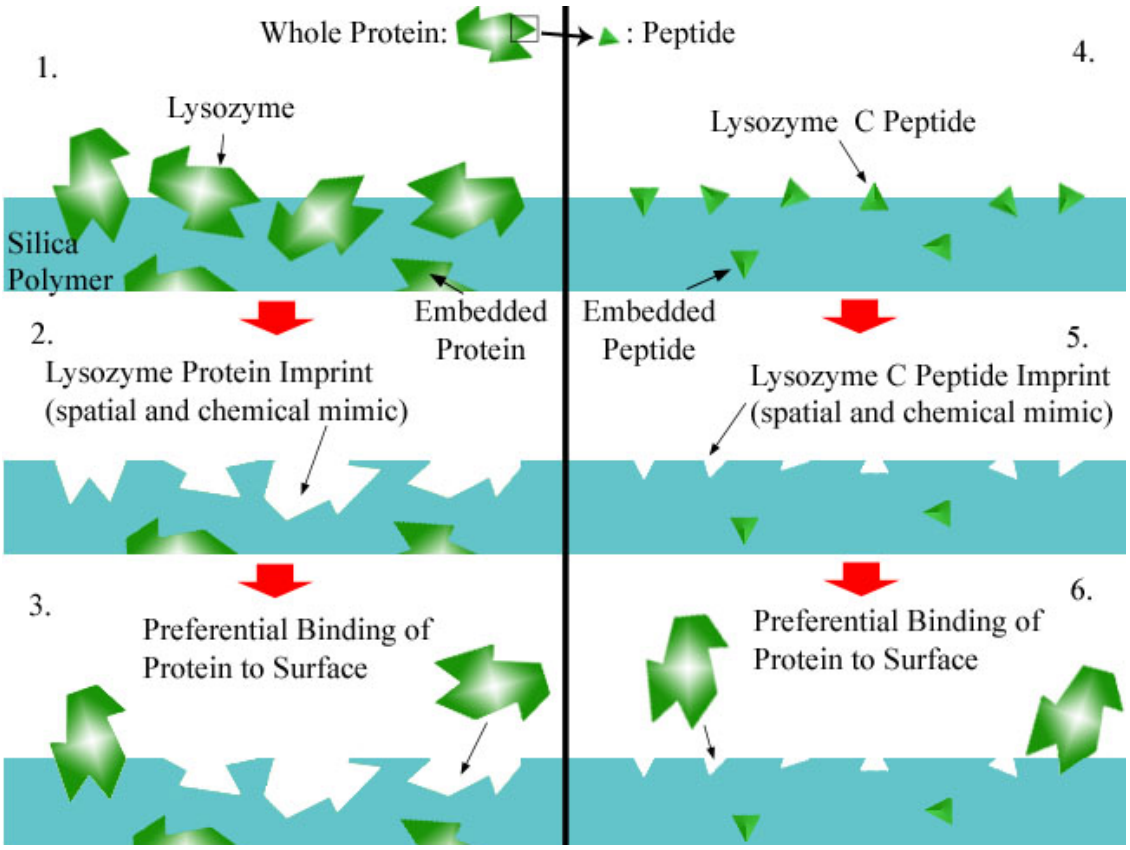

Figure 8. Comparison of whole protein and peptide imprinting on polysiloxane scaffolds.

2.6. Sol-gel Processing

In general, polymers are great materials for use in biological systems because they are stable, biocompatible, can be made of natural components, and have a structure that can be manipulated easily for different applications. Some polymers, such as poly(lactic-co-glycolic acid) (PLGA), can be used in drug delivery as degradable chemical carriers, while other polymers like hydrogels can be used as tissue replacements because of their gel-like properties and high water content. Poly(methylmethacrylate) (PMMA) is a polymer widely used as bone cement because of the strong bonds made during polymerization between an implant material and bone tissue [26].

Polymers make great molecular imprinting materials because of the way they recognize the template molecule. The chemistry of the polymer allows for

organization of the complementary functional groups in the template and the formation of the shape-selective cavity that is complementary to the template [49]. The kind of polymer used and the mechanism in which the template molecule is entrapped and dissociated from the imprint varies widely throughout many studies. Polysiloxanes, a common family of inorganic polymers, are used as excellent MIPs because of their ease of fabrication, good molecule imprinting, and high template recognition. In one study, investigated by Venton and Gutipati [50], it was observed that the silica based monomers tended to associate well with the functional groups on the protein during polymerization. Removal of the protein led to complimentary 'binding pockets' in the polymer that allowed rebinding of the bovine serum albumin (BSA) protein.

Sol-gel processing is one technique used in fabricating amorphous inorganic polymers. The advantage of using sol-gel processing is that integration of the template molecule into the polymer is done easily and the polymerization process takes only a matter of seconds. The term sol-gel comes from the idea of transitioning the liquid mixture solution of colloidal particles (sol) into an interconnected polymer network (gel) [51]. The process requires a mixture of two solutions, the first being a cross-linking agent, and the second containing the functional monomer and template molecule. When the two are combined, the reaction mixture undergoes several polymerization steps [52, 53]. First, a hydrolysis reaction replaces alkoxide groups with hydroxide groups. Next, through alcohol condensation and water condensation, silanol bonds (Si-OH) become siloxane bonds (Si-O-Si) [53] (Figure 9). The growing siloxane bonds create a polymer network through polycondensation that incorporate the functional monomers and template molecules into the bulk material, entrapping water in the process to form a gel. Aging and then drying of the polymer results in evaporation of the liquid and the production of a strong, brittle material [52].

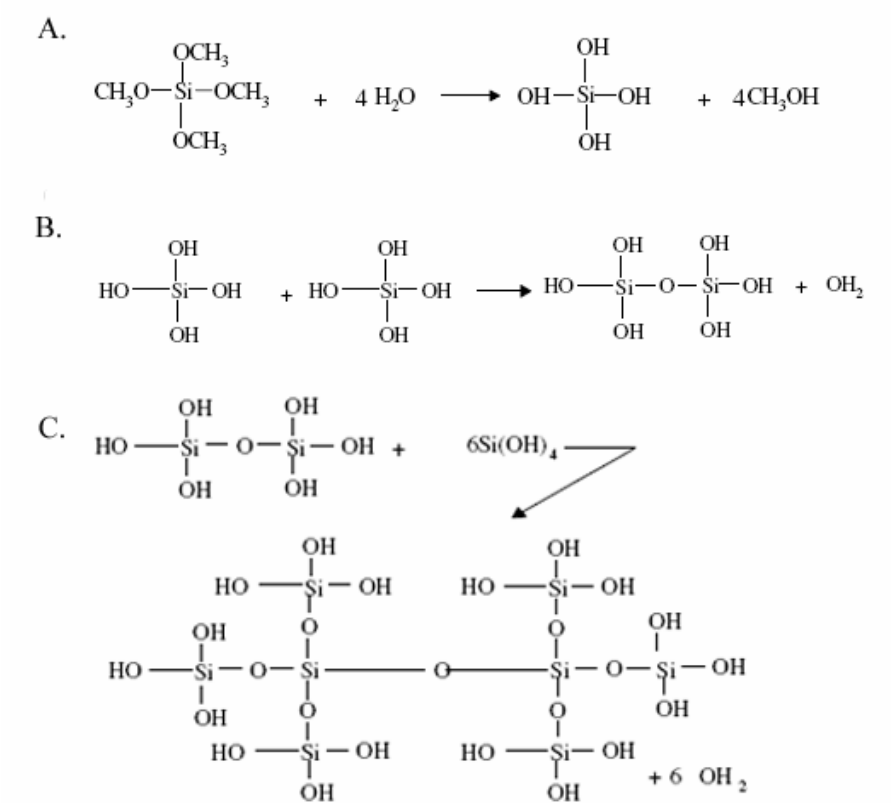

Figure 9. Chemical steps of sol-gel processing to form polysiloxane. A. Hydrolysis of the alkoxide groups. B. Conversion of silanol bonds into siloxane bonds via condensation. C. Polycondensation of alkoxisilanes to form interconnected network [53].

2.7. Significance

While solutions exist for repairing defects in bone tissue due to injury and disease, there is still much room for improvement in this area of medicine. Tissue engineering and bone tissue grafting are current approaches to addressing these problems. In these techniques, bone tissue is replaced by strategically influencing the body's own regenerative abilities instead of using foreign material which may cause complications. In order for bone grafting to be effective, it must utilize the physiological system properly and invoke a controlled biological response. This can be done by altering the properties of the biomaterial at hand to immobilize specific biomolecules for a desired outcome. One way of immobilizing protein on the surface of polysiloxane scaffolds for controlled cellular behavior is by using molecular imprinting. Molecular imprinting

allows specialized crevices to preferentially rebind a template protein because of their complementary spatial and chemical orientation of certain functional groups. Specialized imprints are created from embedding the protein on the surface of the material during polymerization of the polysiloxane and safely digesting it.

Although molecular imprinting has been proven suitable using imprints with small biomolecules, approaches utilizing protein relevant to bone physiology, such as BMP-2, and preferentially binding protein via peptide imprints (the 'epitope' approach), have not been fully explored. Therefore, the objectives of this study were to: 1.) Discern if imprinting polysiloxane scaffolds with a peptide (lysozyme C peptide) could preferentially bind the protein (lysozyme) just as well or better than imprinting with just the protein, 2.) Determine if preferential binding of BMP-2 via imprinting polysiloxane scaffolds can be accomplished, and 3.) Determine if preferential binding of BMP-2 on polysiloxane scaffolds invokes a controlled cellular response.

3. Methods and Materials

3.1. Purifying BMP-2

Bone morphogenetic protein 2 (BMP-2) was used in the study because of its ability to induce osteoblast differentiation and bone formation. BMP-2 (Human Recombinant 85%, 11.989kDa, 1mg, Kamiya Biomedical Company) was found to have contained human serum albumin (HSA). The protein sample must contain only BMP-2 in order to ensure imprinting of purely the template molecule. First, the BMP-2 was suspended in 1mL of 0.1M carbonate-bicarbonate (carb-bicarb) buffer pH 8.5. The solution was then broken up into eight aliquots of 125μL each into small microcentrifuge tubes. The albumin was then removed from the protein samples using the SwellGel Blue Albumin Removal Kit protocol (Pierce). The resulting filtered protein samples were collected into one tube and if necessary suspended to 1mL using carb-bicarb buffer.

3.2. Fluorescent Labeling

In order to determine the amount of protein bound on the surface of the polymer scaffolds, all protein and peptides used in the imprinting experiments were fluorescently labeled with Invitrogen's Amine-Reactive Probes. Lysozyme, BMP-2, and lysozyme C peptide were labeled with Alexa Fluor 350, ribonuclease A (RNase A) and trypsin were labeled with Alexa Fluor 594, and other batches of lysozyme and BMP-2 were labeled with Alexa Fluor 488. Proteins labeled with Alexa Fluor 350 were initially embedded within the polymer scaffolds and later released to quantify the amount that was imprinted on the surface. Proteins labeled with Alexa Fluor 594 were the competitor molecules competing with the template proteins labeled with Alexa Fluor 488 for available surface binding sites.

3.2.1. Labeling Lysozyme C Peptide

The peptide used in the imprinting experiments was Lysozyme C (46-61) (chicken) with a molecular weight of 1753.84Da (Bachem). The peptide was first suspended in 1mL of 0.1M carb-bicarb buffer pH 8.5 to make a 5mg/mL solution. The Alexa Fluor 350 dye was suspended in dimethyl sulfoxide (DMSO) at 1mg/100µL. The Invitrogen protocol called for 50µL of the 10mg/mL dye solution to be mixed with a protein solution of 5-20mg/mL. Since 1mL of a 5mg/mL stock of the peptide was available, only 400µL was used. The 50µL of Alexa Fluor dye was slowly added to the peptide mix. The resulting mixture consisted of 450µL of liquid, which was covered in aluminum foil, shaken, and mixed for one hour in a small 1.5mL centrifuge tube on an orbital shaker in order to allow binding of the fluorescent dye to the protein. Next, the liquid was transferred to a dialysis pouch filter (Slide-A-Lyzer Dialysis Cassette 2000 MWCO 0.2-0.5mL capacity, Pierce) via a 20 gauge syringe. The pouch containing the unfiltered protein solution was suspended in a beaker with a volume of carb-bicarb buffer 500 times the volume of the pouch (225mL) and was left covered in aluminum foil for three periods of 2 hours each. In between periods the outer volume was replaced with fresh carb-bicarb buffer. For the last period, the beaker was placed in a 4°C refrigerator overnight covered in aluminum foil. After dialysis, the labeled peptide was removed via syringe and placed in a 1.5mL centrifuge tube for storage in a -20°C freezer.

3.2.2. Labeling Lysozyme and Bone Morphogenetic Protein 2

Lysozyme protein (from chicken egg white, Sigma) and BMP-2 were labeled much in the same way as the lysozyme C peptide. To suspend the solid protein, 20mg of lysozyme was mixed in 1mL of carb-bicarb buffer to form a concentration of 20mg/mL, while 1mL of carb-bicarb buffer was dispensed in the BMP-2 storage tube. Since lysozyme and BMP-2 are used for imprinting the polymer as well as testing for preferential binding, two different fluorescent labels were tagged to the protein. Aliquots of 50µL of Alexa Fluor 350 and 50µL of

Alexa Fluor 488 were slowly mixed with two separate solutions (four solutions total) of the 20mg/mL lysozyme mix and 250 µL of the BMP-2 stock (after purified of albumin) and shaken for 1 hour covered with aluminum foil at room temperature on an orbital shaker. Once labeled, any leftover unbound amine-reactive probes were filtered out in order to eliminate erroneous protein quantification. The four solutions were transferred to separate larger centrifugal filter tubes (Amicon Ultra – 4 Ultracel – 10k Regenerated Cellulose 10,000 MWCO, Millipore)) and spun in a centrifuge (Marathon 21 K/R, Fisher Scientific) at 3000 rpm and 25°C for three sets of 1 hour time periods. At the end of each period, carb-bicarb buffer was filled to the 1mL mark on the tube so that the non-filtered material was allowed to disperse before being spun once more. This maximized the amount of unbound fluorescent dye to find the filtration pores. After the last period, the newly labeled protein was suspended in 1mL carb-bicarb buffer (if necessary) and stored in the -20°C freezer until use.

3.2.3. Labeling RNase A and Trypsin

Ribonuclease A (type 1-AS from bovine pancreas, 13.7kDa, Sigma) and trypsin (from bovine pancreas, 23.8kDa, Sigma) were used as competitors in rebinding experiments for lysozyme and BMP-2, respectively. Both proteins make great competitors because they are of similar molecular weight and size of the template molecule. RNase A and trypsin were labeled the exact same way as both lysozyme and BMP-2, except that they were labeled with Alexa Fluor 594 and not 488.

3.3. Determining Protein Concentration

The BCA (bicinchoninic acid) protein assay (Pierce) was used to determine the concentration of protein in a solution using colorimetric detection. Even though a protein solution of 20mg/mL may be labeled, some content can be lost during transfer and filtration steps, which can slightly change the total concentration. The assay begins with a simple 1:2 serial dilution of a standard

protein (bovine serum albumin (BSA), Pierce), making a range of dilutions each successively ½ the concentration of the one before it. These dilutions therefore have known concentrations and are used to make a standard curve based on the relationship between each dilution and its corresponding absorbance value. Most often this correlation is best represented as a linear relationship. Any absorbance values therefore that lie on this line and within the upper and lower limits can be interpolated to find a concentration value, meaning that the concentration of a protein sample with a known absorbance value can be accurately estimated. The BCA assay protocol that was followed in the experiment was Pierce's BCA Protein Assay Microtiter plate protocol. Eleven dilutions and one blank of the known BSA protein samples as well as all of the unknown protein samples were transferred into a 96 well culture plate (Costar), which consisted of 10μL of sample and 200μL of working reagent provided in the BCA Protein Assay kit. After incubation at 37°C for 30 minutes, the plate was placed on an absorbance reader (Dynatech MR5000 spectrophotometer), and the absorbance values were obtained by reading at a wavelength of 570nm. Using Microsoft Excel, the standard protein points were plotted (absorbance on the X axis and concentration on the Y), a linear regression curve was found with its equation, and the concentration values from the absorbance measurements of the unknown protein solution were determined. These values (along with dilution factors) were used to come up with an average protein concentration for the entirely labeled and filtered protein batch.

The BCA assay bridges the gap between a protein/peptide's concentration and fluorescence properties. When the protein was labeled with the Alexa dye, there was no way of relating the amount of protein to its fluorescent values alone since the numbers were of an arbitrary scale. Using the BCA assay to determine the protein's concentration and then matching those values to a fluorometric scale enabled a clear translation between fluorescence and amount of protein in the sample.

3.4. Polysiloxane Scaffold Fabrication

The use of polysiloxane in the study was decided upon due to its effectiveness in creating imprinted scaffolds and ease of processing. Fabrication of the polysiloxane scaffolds began with a two step sol-gel (part solution, part gel) process. In step one, 660μL of tetraethoxysilane (TEOS) (Fluka), a cross-linking agent, was mixed with 165μL of 0.1M hydrochloric acid (HCl), 117.5μL of absolute ethanol, and 200μL of distilled water (all per one scaffold) in a 50mL cylindrical tube (Fisherbrand). The vial was then placed on an orbital shaker for 24 hours. In step two, 165μL of γ-aminopropyltriethoxysilane (APS) (Sigma) and 500μL of 0.1M sodium dodecyl sulfate (SDS) were placed in 18mm diameter plastic vials and allowed to stand for 30 minutes at room temperature. The solution was then vortexed briefly to induce small bubbles while 50μL of a labeled protein mix was added via pipetter (Finnpipette II, Fisherbrand). The amount of protein added to each scaffold depended on the type of protein to be imprinted and the amount of that protein available. For lysozyme protein imprinting, 0.1 mg was added. For the lysozyme C peptide imprinting, 0.05mg was added to the scaffolds. For BMP-2 imprinted scaffolds, 0.03mg of protein was added. The bubbles created from SDS agitation give the scaffolds their porous structure. Subsequently, 1140μL of the solution in step one was quickly added to the plastic vials and violently vortexed from 5 to 10 seconds, forming a gel. Blank scaffolds were made without the addition of protein. All samples were capped and aged for 24 hours then uncapped and dried at 40ºC for 48 hours. The aging process allows the gel to set with the embedded protein and water, while incubation dehydrates the gel to form a brittle scaffold.

The scaffolds were then shaped into uniform cylinders using an Ecomet 3 variable speed grinder-polisher with 600 grit silicon carbide papers. Grinding gave the scaffolds a uniform shape and removed the shiny outer layer residue on the tops and bottoms that cover protein binding sites. The final dimensions of the polysiloxane scaffolds were 4mm high and 9mm in diameter. Polymer samples were then rinsed three times with phosphate buffered saline (PBS) pH 7.4. A

pump (ROC-R 115v 4.2amp, Gast) created the vacuum with a Pasteur pipette (5 ¾") on the end of a clear rubber hose. Scaffolds were stored in the multi-well plates covered with aluminum foil until use. The scaffold fabrication process is summarized in Figure 10.

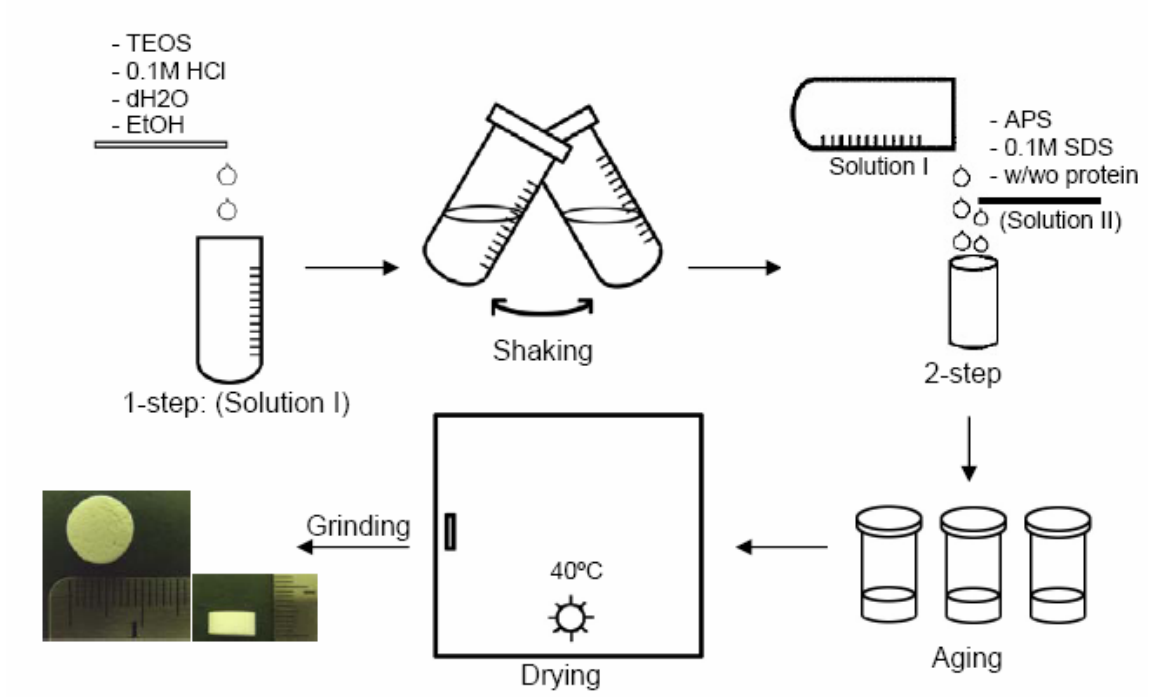

Figure 10. Fabrication process and dimensions of protein imprinted polysiloxane scaffolds. Illustration adopted from the thesis of Kyoungmi Lee, 2005.

3.5. Characterizing Scaffold Maximum Loading Capacity

Polysiloxane scaffolds loaded with labeled protein were characterized by how much protein could potentially rebind based on the amount available on the porous surface. Washing the scaffolds ensured that no proteins were adhering to the surface non-specifically. First, both blank and fully loaded protein scaffolds were organized separately on the flat bottom 24 well plates. An amount of 1mL of a 0.4 mg/mL protease solution (Protease E, Sigma) was then added to each well. The protease digested the protein to allow it and the fluorescent label to diffuse out of the scaffold. In order to quantify the amount of digested protein coming off the scaffold, a standard protein solution was made (similar to a BCA

assay) and compared to the samples in the wells. A small portion of the stock labeled protein obtained after filtration was transferred into a small conical tube and diluted 11 times using 2:1 serial dilutions in similar tubes. The BCA assay previously determined the protein's stock concentration, so each subsequent dilution was determined by dividing the value by one half. Then, 25μL of the serial dilutions as well as the unknown samples were placed in a half area bottom 96 well plate, and were placed in a fluorometric plate reader (Spectra MAX Gemini XS). For Alexa Fluor 350, excitation and emission wavelengths were 346nm and 442nm, respectively. The collected fluorescence values were used to create a regression curve to compare the unknown sample protein concentrations in Microsoft Excel. The protein volumes were measured at 3 and 24 hours after protease addition.

3.6. Preferential Binding Test

The maximum loading capacity value for the polysiloxane scaffolds provides a good estimate of the volume of protein that will be able to rebind to the surface. To test preferential binding of the template on the scaffold, a competitor protein was used with the same size and molecular weight. A true imprint will contain chemical functional groups that complement a unique protein, so even though the competitor molecules may bind non-specifically in the crevice, the template will have a better affinity and the geometry to do so.

The maximum loading amount was converted into moles so that an equal number of template and competitor proteins could compete for the binding sites. With lysozyme or lysozyme C peptide imprinted scaffolds, the competitor was RNase, and likewise with BMP-2 the competitor was trypsin. After digestion of the bound protein from the previous step, the scaffolds were rinsed three times with PBS, pH 7.4. The empty scaffolds were then exposed to 1mL each of a protein-containing solution. Three solutions were added to both imprinted and blank scaffolds: one containing 1mL of the maximum loading amount of template protein, one containing 1mL of the maximum loading amount of competitor, and one with 0.5mL of the template and 0.5mL of the competitor. Each 0.5mL

volume corresponded to half of the maximum loading amount, creating a template to competitor ratio of one to one (1:1). The protein solutions (1:0 (template to competitor), 1:1, and 0:1 of both imprinted and competitor) were allowed 24 hours to bind to the imprinted and non-imprinted scaffolds. Because the proteins were labeled with light sensitive fluorescent markers, the wells were covered with aluminum foil. The plate was placed on an orbital shaker at room temperature for 24 hours.

After 24 hours, the wells were rinsed three times with PBS. Rinsing the scaffolds in this case removed all excess protein that may have been loosely bound to the surface. With no solution in the wells, 1mL of 0.4 mg/mL protease mix was applied to each of the scaffolds. The plate was then recovered and placed on the orbital shaker. Over time, the protease digested the protein that had bound to the scaffold and their components flowed out of the porous structure. The digestion of the proteins does not alter their ability to be detected by fluorometry, so the amount of protein that goes into solution represents the amount that had been preferentially bound. A small sample of each well was taken 48 hours after the protease had been added (the same amount of time the template and competitor were allowed to bind). Each sample was placed in one well of the 96 well, half area plate according to the position of the original wells the scaffolds rested in. The plate was then read using the fluorometric plate reader to find fluorescent values for each sample. Since template and competitor protein binding amounts were compared, both were labeled with different fluorescent markers. The samples therefore were read at two different excitation and emission wavelengths. Alexa Fluor 488 had excitation and emission wavelengths of 495nm and 519nm, respectively, while Alexa Fluor 594 had excitation and emission wavelengths of 590nm and 617nm, respectively. Fluorescent standards for both template and competitor were made using the two respective filtered working stock protein concentrations. Pure stock was serial diluted by one half 11 times (the 12th value was blank buffer) and ran to determine fluorescence values. These values in conjunction with the known protein concentrations allowed a linear regression curve to be made. The

fluorescent values measured from the samples in the wells containing the released protein were then compared with the regression curve to determine approximate concentrations and mass values.

3.7. Statistical Analysis

A two-way analysis of variance (ANOVA) was run using the computer program Graphpad Prism v4.03 to determine statistical significance of the type of protein and ratio groups for lysozyme, BMP-2, and peptide imprinted scaffolds. In addition, Bonferroni post tests were done to determine interaction between the groups. T-tests on the results of the protein imprinted and peptide imprinted scaffolds were done using Graphpad Prism. A power analysis was run using the program Power and Precision release 2.1 to find the number of samples (N) required for obtaining a power of 0.80 for all statistically insignificant data. Alpha for the power analysis was 0.05 with 2 tails. All results are plotted as mean ± standard deviation (SD), unless otherwise specified.

3.8. Cytocompatibility

3.8.1. Preparation

The *in vitro* study consisted of growing cells on blank polysiloxanes scaffolds. Sterilization of the scaffolds involved submerging them in 70% ethanol (dilution of absolute ethanol, Sigma-Aldrich) in a 15mL sterile conical tube and centrifuging them at 1500 rpm for 5 minutes. The scaffolds were then placed in a 6 well plate under a sterile hood without UV light and submerged in 5mL of PBS for 24 hours to diffuse out any harmful residual ethanol. The scaffolds were then allowed to air dry under the hood for 3 hours. The experiment contained three groups: 1.) wells with cells but no scaffolds, 2.) wells with cells on scaffolds, and 3.) wells with no cells but containing scaffolds. C3H/10T1/2 (C3H; CCL-226, ATCC Rockville, MD) cells were cultured and passaged in T-75 cell culture flasks (Corning; Corning, NY). An amount of 100,000 cells were seeded directly on the scaffolds or onto the floor of the tissue culture wells in a volume of 270μL and

incubated for 2 hours to allow for infiltration and attachment. Phenol red free medium (Minimum Essential Medium Alpha, Gibco) with 10% heat-inactivated fetal bovine serum (FBS) was added to each well in 5mL aliquots. Cell-free wells contained scaffolds immersed only in aMEM + 10% FBS. Samples were then incubated for 1, 3, and 7 days, during which they were subjected to a deoxyribonucleic acid (DNA) assay to determine DNA content.

3.8.2. Determining Deoxyribonucleic Acid Content

The amount of DNA was determined using the Hoechst 33258 assay to test the cytocompatibility of the scaffolds. Scaffolds that were seeded with C3H cells were washed with warm PBS twice, and then submerged in 1mL of high salt buffer (pH 7.4, containing 0.05M NaH_2PO_4, 2M NaCl and 2 mM EDTA). All wells, including those without scaffolds and only cells, were sonicated and stored in the freezer for later use. Once all samples were collected for each time period (1, 3, and 7 days), the lysates were centrifuged to separate disintegrated scaffold materials from the DNA-containing supernatant using an Eppendorf 5145 centrifuge. Two-fold serial dilutions of calf thymus DNA were made in the high salt buffer for running a standard curve to determine the unknown DNA concentrations in each well. Each sample, including the two-fold standard amounts, was added to a 96 well plate. An amount of 50µL of Hoechst 33258 reagent per 200µL of DNA supernatant was added to each sample and covered in the dark for 10 minutes. Fluorescence was measured at 356nm excitation and 458nm emission using a fluorometric plate reader.

4. Results

4.1. Fabrication of Scaffolds

The polysiloxane scaffolds created in the present study were cylinders with dimensions of 4mm in height and 9mm in diameter. The scaffolds had a bright white color, and after hardening became very brittle and porous (Figure 11). In a previous experiment [54], the average pore size for the scaffolds was found to be 6.19μm, while the average porosity was 43%. Throughout most of the experiments, the scaffolds retained shape and porosity except for a few instances where degradation occurred during long immersion periods (greater than 120 hours).

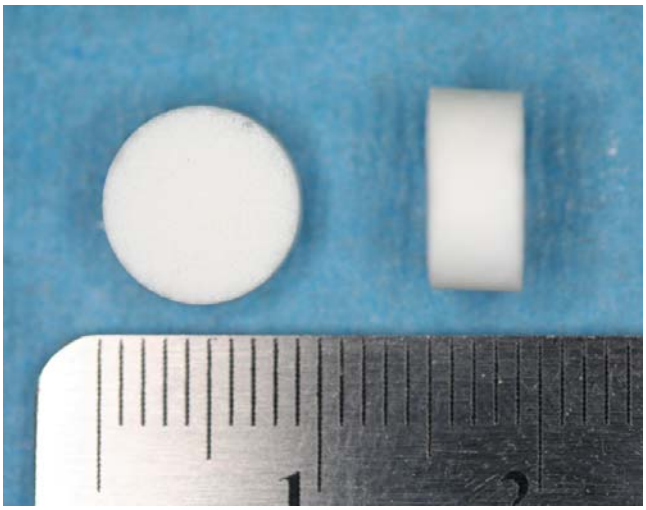

Figure 11. Dimensions of the fabricated porous polysiloxane scaffolds.

During polymerization, 50μL of protein was inserted in the vial just before step 1 and 2 solutions were mixed together. As the mix was vortexed, the liquid within a matter of seconds became gelatinous. During that short period, however, the liquid splashed around and separated from the bulk which created random spots on the sides of the tube. As the polymer aged and dried in the oven, much of the polymer remained as a residue on the sides and on the bottom of the container. When removed from the tube, the shape of the polymer on the top was not perfectly flat due to the vortexing step. The side surface and bottom

however were circular and flat, respectively. Grinding of the scaffold, therefore, was necessary to reshape the scaffolds into uniform cylinders in addition to removing the glassy surface on the tops and bottoms.

To compensate for such large protein losses and therefore reduced number of imprints, the scaffold protein density was increased. This was done by adding a higher mass of protein and reducing the polymer volume to two-thirds of the original. Polymerization was achieved using two-thirds of the original volume of each component. For instance, only 760μL (originally 1140μL) of step one was added to step two, which itself consisted of 110μL APS and 333μL of SDS (originally 165μL of APS and 333μL of SDS). The result was a scaffold approximately two thirds the size of the original but with the same characteristics. The dried polymer residue on the sides of the tube was still present, and after grinding, the dimensions were 3.35mm in height and 8.4mm in diameter (compared to the original 4mm by 9mm).

4.2. Protein Maximum Loading Capacity

4.2.1. Comparison of Protein to Peptide

After the polysiloxane scaffolds embedded with protein were fabricated and shaped into cylinders, they were exposed to 1mL of a 0.4mg/mL protease mix. The protease digested all of the protein it came in contact with, suggesting the protein on the direct surface within the porous structure was affected. When the protein was broken down, its complementary chemical and spatial arrangement was left exposed. Therefore, a direct correlation was made between protein digested from the scaffold and the amount of imprinting sites available for preferential rebinding of the same protein. Amounts of digested lysozyme protein were determined using a fluorometric reader for 3, 24, 48, and 96 hours after the addition of the enzyme. It was found that beyond 24 hours the rate of protein unloading from the scaffold was relatively small and therefore not considered in the analysis (Figure 12). This was used as a guide for the proceeding maximum unloading experiments which involved the release of lysozyme protein and lysozyme C peptide.

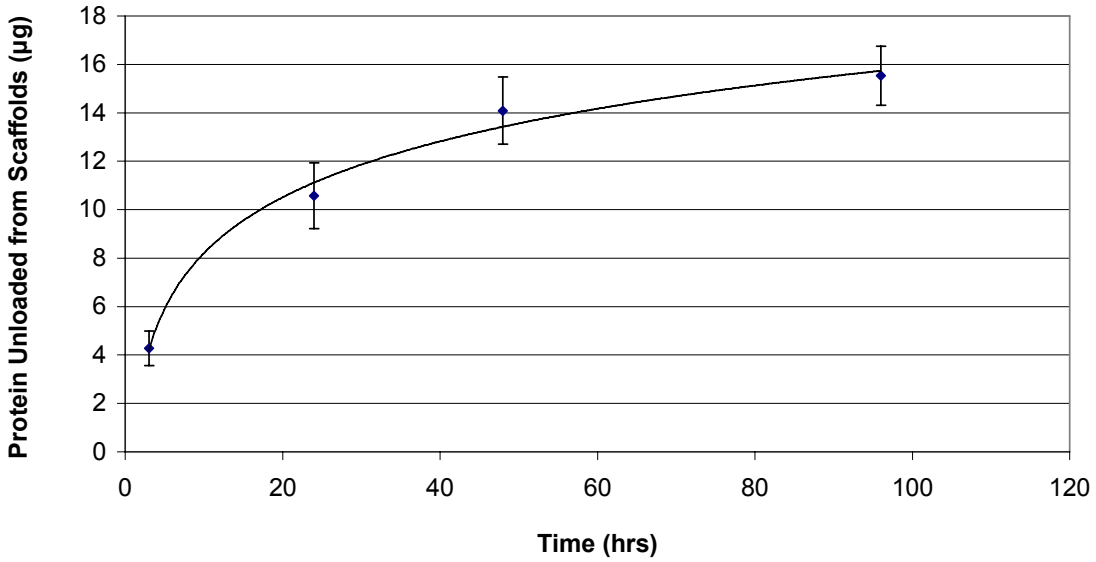

Figure 12. Release rate of protein from scaffolds as a function of time following protease addition. The level of protein release slowed after 24 hours (mean ± SD of 10.57 ± 1.36, n=7).

Figure 13 shows the maximum loading capacity for the lysozyme imprinted scaffolds, and Figure 14 shows the capacity values for the lysozyme C peptide imprinted scaffolds. In this instance, 0.1mg of lysozyme protein and 0.05mg of peptide was added to the polymerization mix. Because a larger amount of protein was used to make the lysozyme imprinted scaffolds, a greater amount was recorded leaving the protein scaffold than leaving the peptide scaffold. The protein amounts recorded at 3 hours and 24 hours after protease addition were found to be statistically different ($p<0.001$) for both protein and peptide imprinted scaffold groups. In addition, at 3 and 24 hours, values were statistically different between both protein and peptide imprinted groups ($p<0.001$). Again, no data past 24 hours was recorded since the amount released topped off around this time.

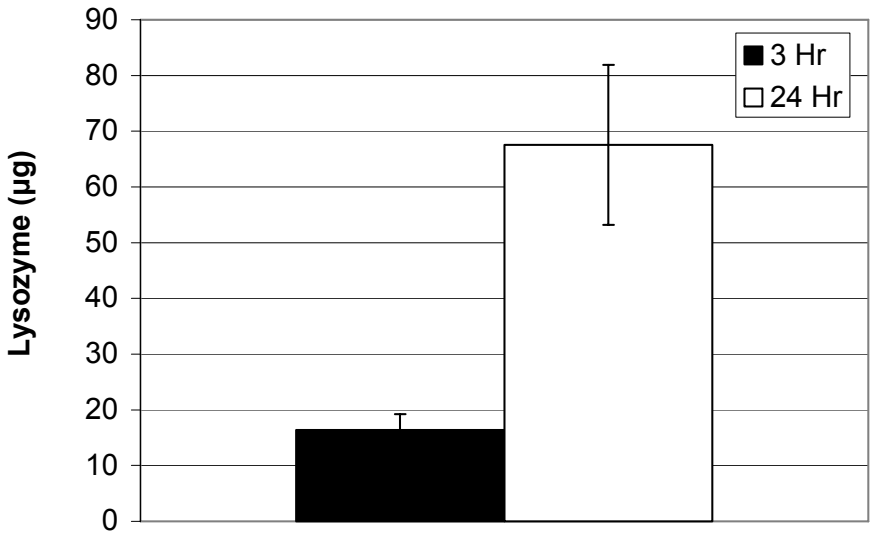

Figure 13. The amount of protein released (mean ± SD) from lysozyme imprinted scaffolds via digestion with 0.4mg/mL of protease after 3 and 24 hours.

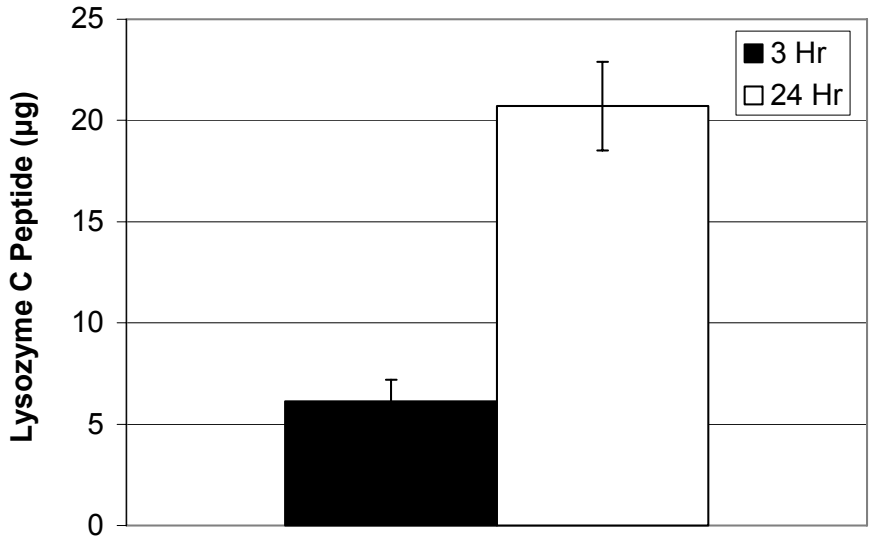

Figure 14. The amount of peptide released (mean ± SD) from lysozyme C peptide imprinted scaffolds via digestion with 0.4mg/mL of protease after 3 and 24 hours.

In Table 1, the mass percentage of the amount of initial added protein/peptide that was released from the scaffolds is shown. A larger amount of protein was removed from the protein imprinted scaffold from the peptide

imprinted scaffold (67.93μg compared to 21.76μg), resulting in a higher percentage for the former.

Table 1. Results of the maximum loading capacity for protein and peptide imprinted scaffolds (mean ± SD).

	Lysozyme	Peptide
Number of Scaffolds (n)	4	12
Amount of Protein Added to Polymerization Mix (μg)	100.00	50.00
Average Amount of Protein Released from Scaffold (μg) (24 hr)	67.65 ± 14.38	20.71 ± 2.18
Percent Protein that forms Imprints	67.65 ± 14.38	41.40 ± 1.45

4.2.2. Variation in Volume of Scaffold

With the idea of increasing the number of binding sites while minimizing protein losses from fabrication, the volume of polymerization mix was reduced to two-thirds normal. Adding a higher amount of protein to a smaller volume of polymer could increase the density and distribution of potential binding sites throughout the scaffold. Figure 15 shows the maximum loading capacity for scaffolds imprinted with lysozyme C peptide with the normal volume, and Figure 16 shows the loading capacity for the two-thirds volume scaffolds imprinted with the peptide. An amount of 0.0174mg of peptide was loaded into the normal volume scaffolds made, while 0.026mg of peptide was loaded into the two-thirds volume scaffolds. Also, the normal scaffolds were polymerized in 18mm diameter tubes while the two-thirds volume scaffolds were polymerized in 15mm glass tubes. The smaller diameter tube was used to enhance the shrinkage of the dimensions of the partial volume scaffolds during polymerization.

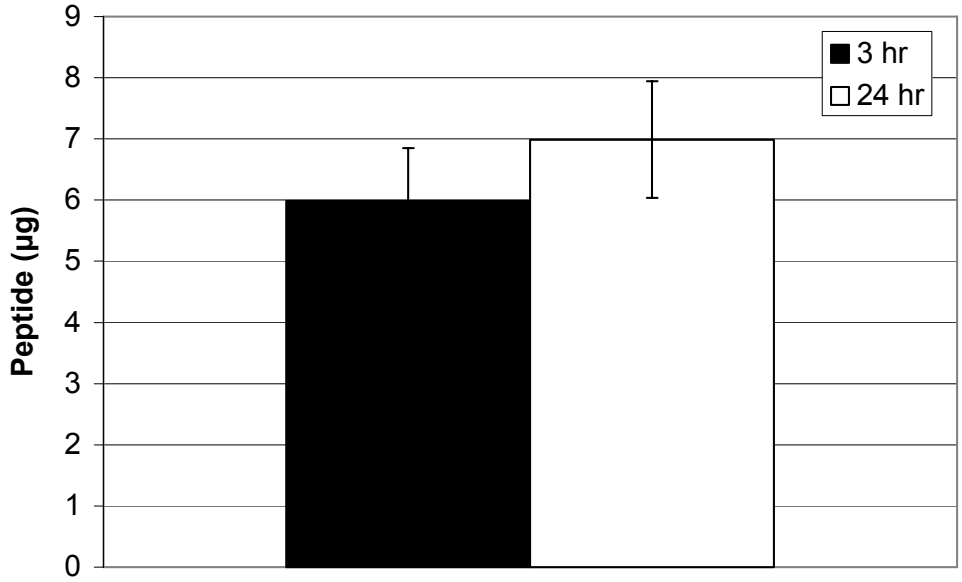

Figure 15. The amount of peptide released (mean ± SD) from full volume lysozyme C peptide imprinted scaffolds via digestion with 0.4mg/mL of protease after 3 and 24 hours.

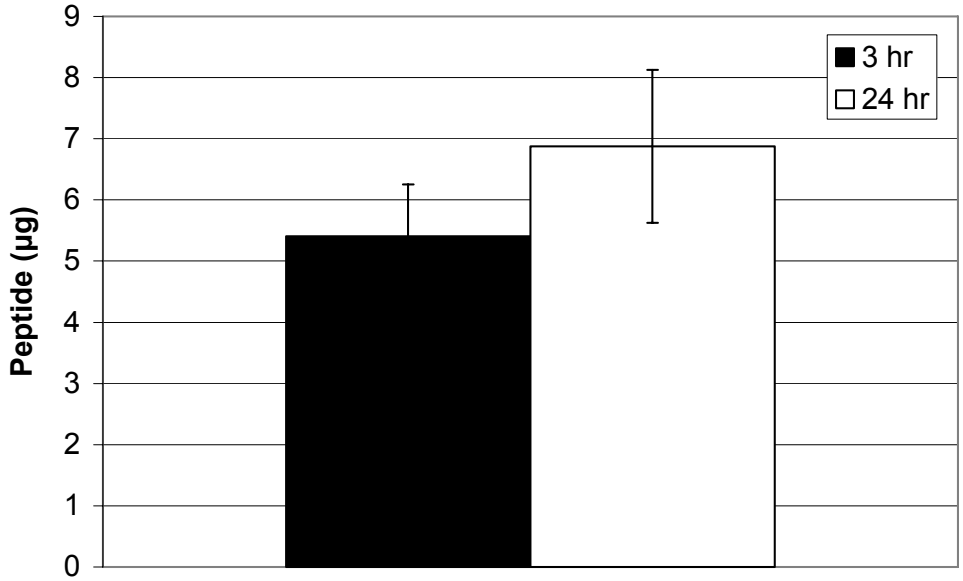

Figure 16. The amount of peptide released (mean ± SD) from partial volume lysozyme C peptide imprinted scaffolds via digestion with 0.4mg/mL of protease after 3 and 24 hours.

Table 2 shows the amounts and percentages of the released peptide after 24 hours. It appears that an increase in the initial peptide amount and a decrease in polymerization mix volume resulted in no quantifiable difference between the release of partial and full volume scaffold peptides. The released protein amount between 3 hours and 24 hours was found to be statistically different ($p<0.05$) after protease addition for both full and partial volume scaffold groups. However, the values at 3 hours between the full and partial groups were not significantly different ($p>0.05$), likewise with the values at 24 hours. While the amount of peptide digested by the protease remained the same for both groups, the percentage of peptide was higher for the full volume scaffolds than for the partial volume scaffolds.

Table 2. Results of the maximum loading test for both full and partial volume peptide imprinted scaffolds (mean ± SD).

	Full Volume	Partial (2/3) Volume
Number of Scaffolds (n)	9	12
Volume of Scaffold (mm^3)	1017.9	742.6
Amount of Peptide Added to Polymerization Mix (μg)	17.40	26.00
Average Amount of Peptide Released from Scaffold (μg) (24hr)	6.99 ± 0.95	6.88 ± 1.25
Percent Peptide that forms Imprints (%) (24hr)	40.16 ± 5.49	26.45 ± 4.81

4.2.3. BMP-2

BMP-2 protein was also used to make imprints in the polysiloxane scaffolds. After digesting in 0.4mg/mL protease, the amount of protein released from the scaffolds was measured using a fluorometric plate reader at three and twenty four hours. Figure 17 shows the amount of BMP-2 that was embedded in

the surface of the scaffold, digested, and released via the protease. The amount of BMP-2 added to the polymerization mix was 0.025mg. The amount of protein determined was used to approximate the amount of molecules that can potentially rebind to the newly made imprints. Table 3 shows the amount of BMP-2 released after 24 hours and the percentage of total protein digested out of the scaffold and used to make imprints. The protein amount for 3 hours and 24 hours was found statistically different ($p<0.001$) after protease addition for the BMP-2 imprinted scaffold group.

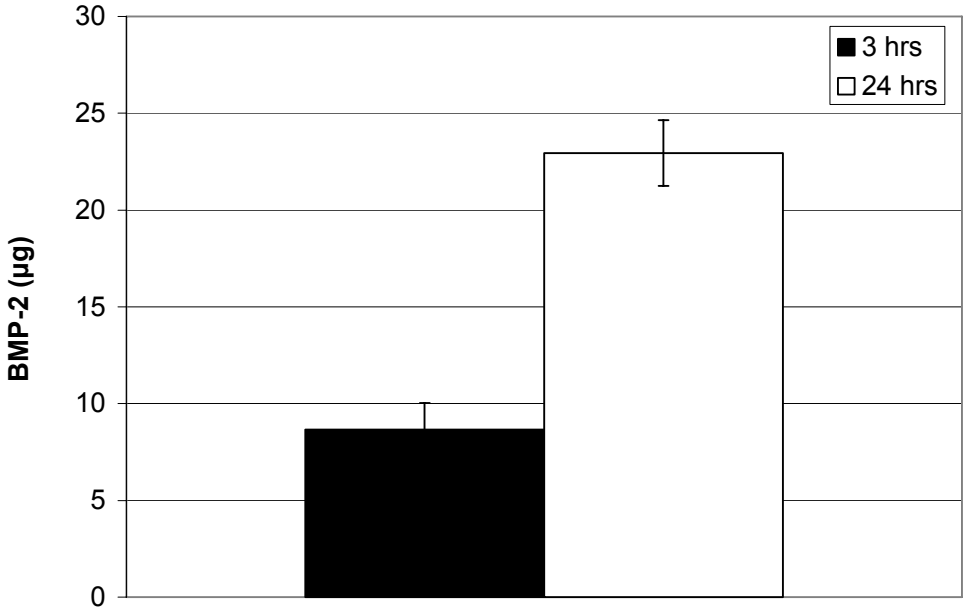

Figure 17. The amount of protein released (mean ± SD) from BMP-2 imprinted scaffolds via digestion with 0.4mg/mL of protease after 3 and 24 hours.

Table 3. Results of the maximum loading capacity for BMP-2 imprinted scaffolds.

	BMP-2
Number of Scaffolds (n)	15
Amount of Protein Added to Polymerization Mix (µg)	30.00
Average Amount of Protein Released from Scaffold (µg) (24hr)	22.95 ± 1.70
Percent of Protein that forms Imprints	74.13 ± 5.66

4.3. Protein Preferential Binding

4.3.1. Lysozyme Imprinted Scaffolds

To test the principles of molecular imprinting with proteins and develop a standard for comparison, lysozyme was imprinted onto polysiloxane scaffolds and tested for preferential binding. At 24 hours, the amount of released protein was approximately 67µg (see Table 1). This amount corresponded to approximately 4.5 x 10^{-9} moles of lysozyme protein molecules. Assuming that this number equaled the number of imprints on the scaffolds, approximately 62µg of RNase A and 67µg of lysozyme were added to each well with a 0:1 and 1:0 ratio, respectively. For the 1:1 ratio wells, 31µg of RNase A and 33.5µg of lysozyme were added. The protein was allowed 24 hours to bind to the scaffolds and another 24 hours to digest via protease. Figure 18 shows the average difference in the actual amount of protein between the imprinted and blank scaffold types. Figure 19 shows the average difference in the imprinted and blank scaffold types in terms of percent bound.

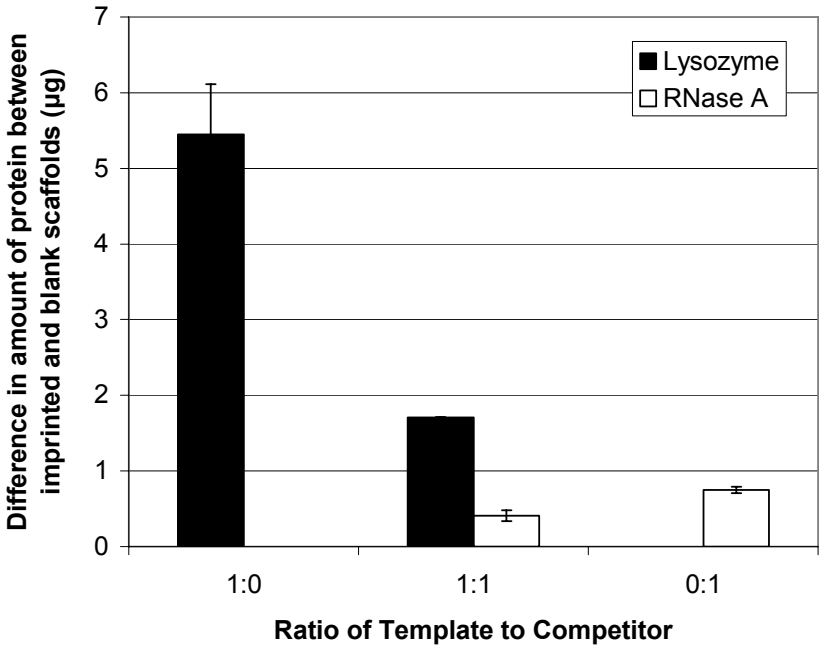

Figure 18. Results of the preferential binding (mean ± SD) on lysozyme imprinted scaffolds based on amount of protein.

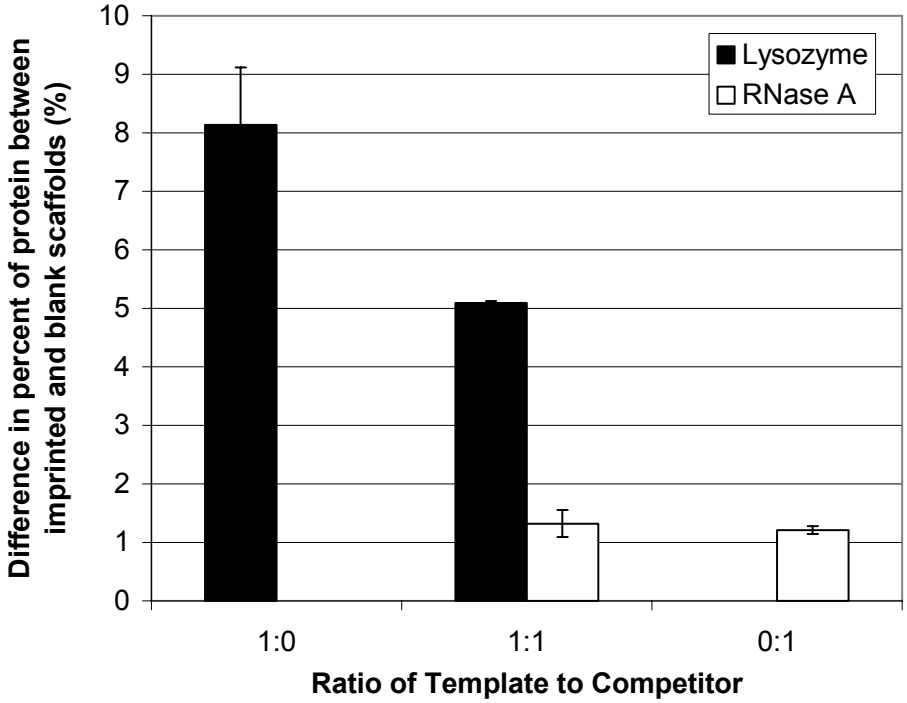

Figure 19. Results of the preferential binding (mean ± SD) on lysozyme imprinted scaffolds based on the percentage of protein.

These figures show that there was more binding of the lysozyme protein to the imprinted scaffolds than the binding of RNase A under both a competitive ($p<0.01$ for amount and $p<0.001$ for %) and noncompetitive environment (a ratio of 1:0 and 0:1) ($p<0.001$ for amount and %). Figure 18 shows that when an equal number of template and competitor protein molecules (1:1 ratio) were added to wells containing the scaffolds, more than 4:1 of lysozyme to RNase preferentially bound the polymer ($p<0.01$).

Table 4 summarizes the amounts and percentages of lysozyme and RNase A that bound to the imprinted and blank scaffolds. Since a certain portion of protein bound the blank scaffold non-specifically, this amount was subtracted from the imprinted scaffold data to isolate only the protein that adhered to the scaffold specifically via protein imprinting. Under competition (1:1 ratio), lysozyme bound about 5.1 ± 0.03% (mean ± SD) of the original amount

deposited in the wells due to protein imprinting, while RNase A bound only 1.32 ± 0.23% of the original.

Table 4. Summary of the preferential binding tests for lysozyme protein imprinted scaffolds (mean ± SD).

Average Protein Bound to Protein Imprinted Polysiloxane Scaffolds (n=3 for each ratio)						
	Lysozyme			RNase A		
Ratio	1:0	1:1	0:1	1:0	1:1	0:1
Imprinted Scaffolds						
Amount Added (μg)	67.00	33.50	0	0	31.00	62.00
Amount Rebound (μg)	8.46 ± 0.00	3.25 ± 0.00	0	0	1.32 ± 0.00	2.78 ± 0.00
Blank Scaffolds						
Amount Added (μg)	67.00	33.50	0	0	31.00	62.00
Amount Rebound (μg)	3.01 ± 0.00	1.54 ± 0.00	0	0	0.91 ± 0.00	2.03 ± 0.00
Difference (Imprinted minus Blank)						
Amount Rebound (μg)	5.45 ± 0.66	1.71 ± 0.01	0	0	0.41 ± 0.07	0.75 ± 0.04
Percent Rebound (%)	8.13 ± 0.99	5.10 ± 0.03	0	0	1.32 ± 0.23	1.21 ± 0.06

4.3.2. Lysozyme C Peptide Imprinted Scaffolds

Many polysiloxane scaffolds were imprinted with lysozyme C peptide, a small amino acid sequence found on the surface of the lysozyme protein. It is desired that the peptide imprint bind the protein to the same degree that it is bound using the imprint of the entire structure. In a separate experiment it was found that the amount of peptide released from the scaffolds in 24 hours was 7.4μg (note: this is not the same batch of scaffolds from which the value of 21μg was obtained (Table 1)). The number of moles of lysozyme C peptide in 7.4μg was 4.22×10^{-9}, suggesting that potentially the same number of lysozyme proteins can bind the surface where the peptide imprints were created. An amount of 4.22×10^{-9} moles corresponded to 0.061mg of lysozyme (template) and 0.058mg of RNase A (competitor). In this circumstance the template and competitor were the same as with the lysozyme imprinted scaffolds. As before,

the 24 well plate contained imprinted and blank (non-imprinted) scaffolds with groups representing a template to competitor ratio of 1:0, 1:1, and 0:1. Figure 20 and Figure 21 show the protein amounts and percentages, respectively, where the blank has been subtracted from the imprinted scaffolds. Interestingly, the standard deviation error bars are so large that the data could suggest there is no difference in preferential binding for the lysozyme. There appears to be a difference between binding under noncompetitive conditions ($p<0.05$ for amount and $p>0.05$ for %), but during competition the two proteins seemed to have bound the same amount. After statistical analysis, this indeed was found to be the case ($p>0.05$ for amount and %).

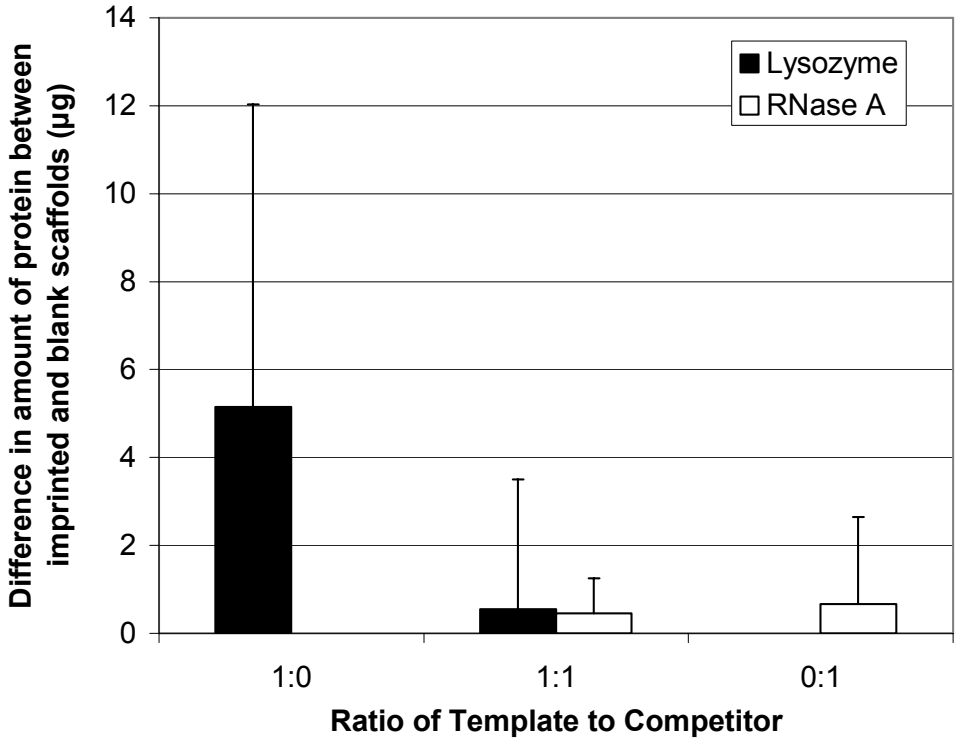

Figure 20. Results of the preferential binding (mean ± SD) on peptide imprinted scaffolds based on the amount of protein.

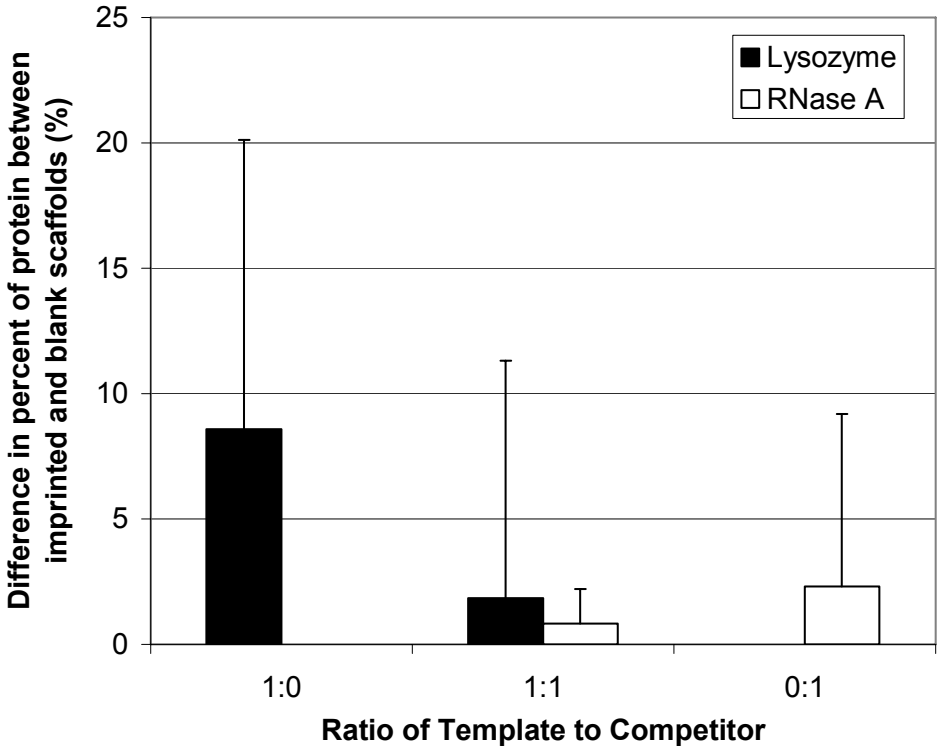

Figure 21. Results of the preferential binding (mean ± SD) on peptide imprinted scaffolds based on the percentage of protein.

Table 5 summarizes the percentages and amounts of lysozyme and RNase A that bound to the peptide imprinted and blank scaffolds. Since a certain portion of protein bound to the blank scaffolds non-specifically, this amount was subtracted from the imprinted scaffold data to isolate the protein that adhered to the scaffold specifically via protein imprinting. Under competition (1:1 ratio), lysozyme bound about 1.85 ± 9.47% (mean ± SD) of the original amount deposited in the wells due to protein imprinting while RNase A bound 0.83 ±1.39% of the original. Unexpectedly, the standard deviations for the peptide imprinted data are unusually high. A power analysis was run to determine the appropriate sample size of imprinted scaffolds needed for a significant difference between template and competitor binding on the 1:1 level. For n=11 and an approximate mean and SD of 0.55 ± 2.95μg for lysozyme and 0.45 ± 0.79μg for RNase A, a sample size of 7,322 would be needed to produce a power of 0.80.

Table 5. Results for the preferential binding tests (mean ± SD) of protein adsorption on lysozyme C peptide imprinted polysiloxane scaffolds.

Average Protein Bound to Peptide Imprinted Polysiloxane Scaffolds (n=11 for each ratio)						
	Lysozyme			RNase		
Peptide Imprinted Scaffolds	1:0	1:1	0:1	1:0	1:1	0:1
Amount Added (μg)	61.00	30.50	0	0	29.00	58.00
Amount Rebound (μg)	26.32 ± 4.81	12.28 ± 4.00	0	0	9.17 ± 1.28	21.03 ± 2.56
Blank Scaffolds						
Amount Added (μg)	61.00	30.50	0	0	29.00	58.00
Amount Rebound (μg)	21.16 ± 8.50	11.74 ± 3.68	0	0	8.72 ± 1.63	20.36 ± 2.40
Difference (Peptide Imprinted minus Blank)						
Amount Rebound (μg)	5.15 ± 6.88	0.55 ± 2.95	0	0	0.45 ± 0.79	0.67 ± 1.98
Percent Rebound (%)	8.59 ± 11.54	1.85 ± 9.47	0	0	0.83 ± 1.40	2.31 ± 6.87

4.3.3. Comparison of Protein to Peptide Imprinted Scaffolds

In addition to looking at the groups of protein imprinted scaffolds and peptide imprinted scaffolds individually, a comparison was made to identify if one type of scaffold preferentially binds a different amount of protein than the other. Statistical analysis was used to compare significant differences in means between the two scaffold types under the non-competitive case (1:0 and 0:1) and competitive case (1:1). In the 1:0 case, no statistical difference in lysozyme binding between protein and peptide imprinted scaffolds was determined. In the 0:1 ratio case, it was determined that no statistical difference in RNase A binding between the two scaffold types existed. In the 1:1 ratio case for lysozyme binding, no statistical difference between protein and peptide imprinted scaffolds was found. Also, for RNase A binding in the 1:1 ratio case, no statistical difference between protein and peptide imprinted scaffolds had occurred. In other words, there was no difference in the amount of protein that binds the protein imprinted scaffolds and peptide imprinted scaffolds in all cases ($p>0.05$).

In each comparison of the scaffold types, a power analysis was used to determine the number of samples required to obtain a power of 0.80. Table 6 below summarizes the results of each statistical comparison with the required number of samples for the desired power. In comparison 1 and 2, both lysozyme and RNase A binding are compared under noncompetitive conditions between peptide and protein imprinted scaffolds. In order for a significant difference in binding to be observed for lysozyme and RNase A, 4,130 scaffolds and 4,881 scaffolds need to be fabricated, respectively. Under competition, 3,087 scaffolds are necessary to see a difference in RNase A binding between the two types of scaffolds, while only 52 scaffolds are necessary for lysozyme.

Table 6. Summary of the statistical comparison of protein that bound to protein and peptide imprinted scaffolds.

		Comparison 1	Comparison 2	Comparison 3	Comparison 4
	Type of protein	Lysozyme	RNase A	Lysozyme	RNase A
	Ratio (Template vs Competitor)	1:0	0:1	1:1	1:1
Protein Imprinted	Mean (μg)	5.45	0.75	1.71	0.41
	Standard Deviation (μg)	0.07	0.04	0.01	0.07
Peptide Imprinted	Mean (μg)	5.15	0.67	0.55	0.45
	Standard Deviation (μg)	6.88	1.98	2.95	0.79
	p value	p>0.05	p>0.05	p>0.05	p>0.05
	Significant Difference?	No	No	No	No
	Desired Power	0.8	0.8	0.8	0.8
	N required for desired power	4,130	4,811	52	3,087

4.3.4. BMP-2 Imprinted Scaffolds

BMP-2 is a key player in the differentiation of osteogenic bone cells and bone formation. BMP-2 was imprinted into polysiloxane scaffolds because of its promising potential for bone regeneration and wound healing. The BMP-2 imprinted scaffolds were exposed to protease in the same manner as the

lysozyme scaffolds for 24 hours, and a release amount of 23μg was measured using a fluorometric plate reader. The amount of template (BMP-2) and competitor (trypsin) added to the 1:0 and 0:1 protein mixes, respectively, were both 23μg. Since both trypsin and BMP-2 have a very similar size (MW), an equal amount of both were placed in the wells. For the 1:1 ratio wells, 0.5mL of both 23μg protein mixes (11.5μg each) were placed in the wells. The results of the amount of protein released from the BMP-2 imprinted scaffolds are shown in Figure 22 for the amount of protein bound and Figure 23 for the percentage bound. Both figures show a noticeable binding of BMP-2 to scaffolds at the 1:0 ratio, as well as a very small but equal amount on scaffolds with a 1:1 ratio, and a negative value for the 0:1 ratio. The standard deviation bars are quite large for all scaffold types. Under noncompetitive conditions, a difference in protein binding can be seen ($p<0.001$ for amount and percent bound), which is enhanced by the negative value for amount of competitor bound. Under the competitive case, the data suggest that there was no preferential binding of BMP-2 on imprinted scaffolds compared to blank, while statistical analysis shows this to be true ($p>0.05$ for amount and %).

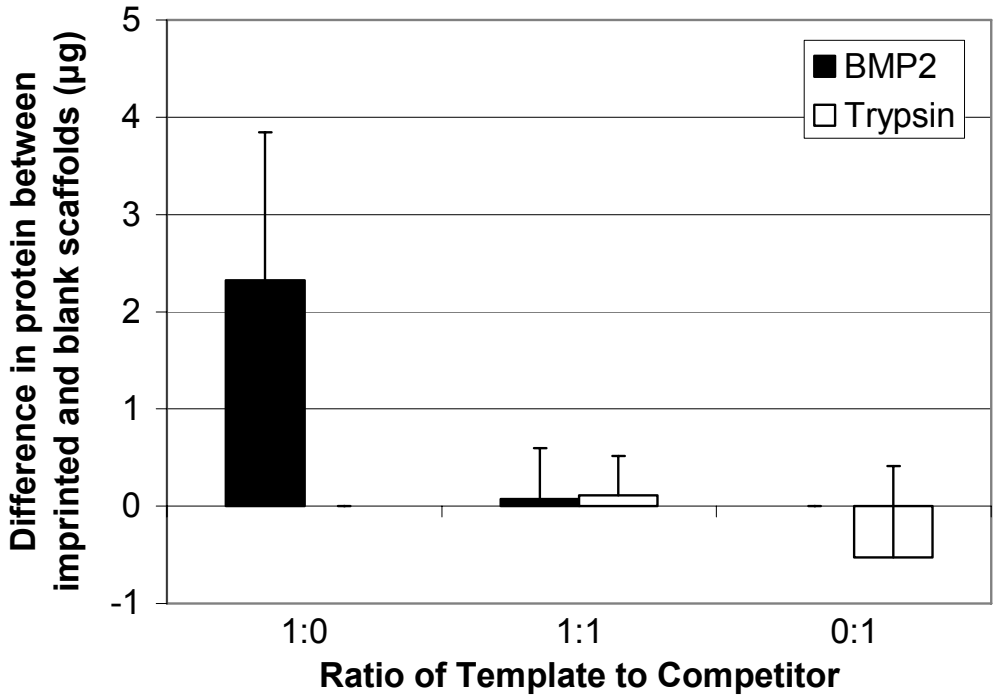

Figure 22. Results of the preferential binding (mean ± SD) on BMP-2 imprinted scaffolds based on the amount of protein.

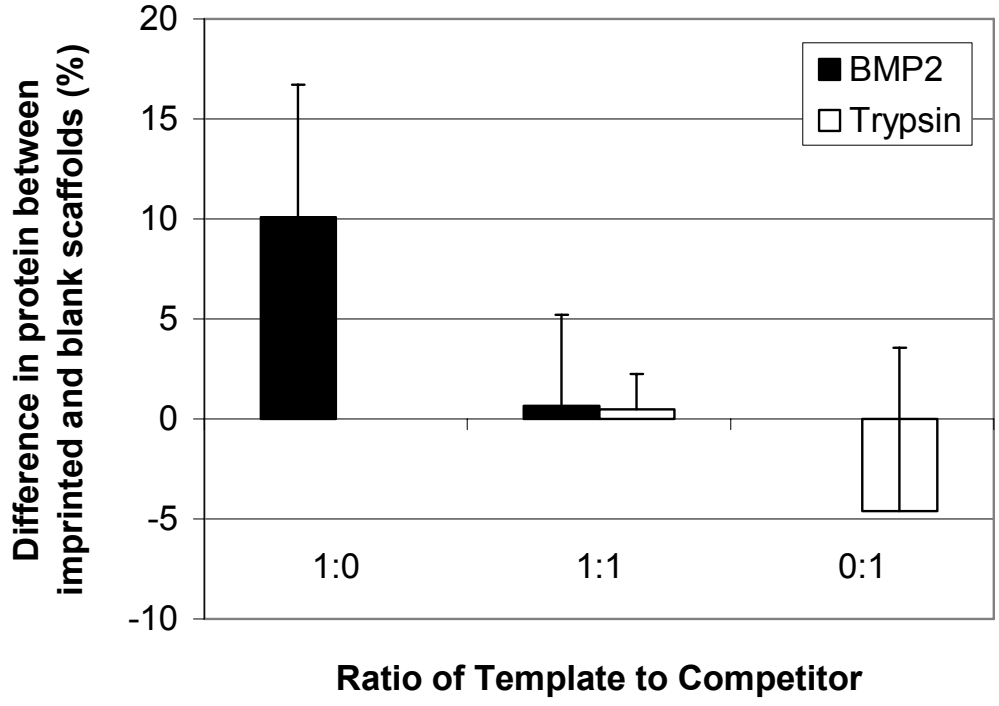

Figure 23. Results of the preferential binding (mean ± SD) on BMP-2 imprinted scaffolds based on the percentage of protein.

Table 7 summarizes the percentages and amounts of BMP-2 and trypsin that bound to the BMP-2 imprinted and blank scaffolds. The results presented in the table as well as the figures pertaining to BMP-2 are similar to the experiments completed with the lysozyme protein and peptide in that the standard deviations are extremely high. Under competition, the BMP-2 imprinted scaffolds bound a very small 0.65 ± 4.55% of the original amount deposited in the wells due to protein imprinting while trypsin bound 0.49 ± 1.77% of the original. A power analysis was run to determine the appropriate sample size of imprinted scaffolds needed for a significant difference between template and competitor binding on the 1:1 level. For n=13 and an approximate mean and SD of 0.08± 0.52μg for lysozyme and 0.11± 0.41μg for RNase A, a sample size of 3,826 would be needed to produce a power of 0.80.

Table 7. Results for the preferential binding tests of protein adsorption on BMP-2 imprinted polysiloxane scaffolds.

Average Protein Bound to BMP-2 Imprinted Polysiloxane Scaffolds (n=13 for all ratios)						
	BMP-2			Trypsin		
BMP-2 Imprinted Scaffolds	1:0	1:1	0:1	1:0	1:1	0:1
Amount Added (μg)	23.00	11.50	0	0	23.00	11.50
Amount Rebound (μg)	12.25 ± 6.33	5.16 ± 3.92	0	0	1.59 ± 0.30	3.00 ± 0.42
Blank Scaffolds						
Amount Added (μg)	23.00	11.50	0	0	23.00	11.50
Amount Rebound (μg)	10.47 ± 7.58	5.10 ± 4.01	0	0	1.48 ± 0.28	3.47 ± 1.33
Difference BMP2 (Imprinted minus Blank)						
Amount Rebound (μg)	2.32 ± 1.52	0.08 ± 0.52	0	0	0.11 ± 0.41	-0.53 ± 0.94
Percent Rebound (%)	10.09 ± 6.62	0.65 ± 4.55	0	0	0.49 ± 1.77	-4.60 ± 8.16

4.4. Cytocompatibility

4.4.1. Preparation

Non-imprinted polysiloxane scaffolds were investigated for their ability to sustain cell viability for one week. While seeding the polymer scaffolds, some of the medium containing the cells spilled over the top surface edge and onto the bottom of the tissue culture plastic well. The condition of these cells was used to observe the effects caused by the scaffold in its immediate vicinity (10-20 μm). On days 4 through 7, spread cells were seen in small groups where they had first settled on day 1 after seeding. These cells, however, were not grown on the scaffolds, and therefore were not included in the proceeding results.

4.4.2. C3H Cell Growth

The ability for cells to grow on the blank polysiloxanes scaffolds was determined by quantifying the amount of DNA present at 1, 3, and 7 days. The number of cells present is related to the quantity of DNA determined using the DNA assay. The results of the DNA analysis are shown in Figure 24 after an initial amount of 100,000 cells was seeded on the surface of either the tissue culture plastic or the porous polymer scaffold. Throughout the entire week of incubation, the amount of DNA present on tissue culture plastic at the bottom of the plate exceeded the amount grown on the polymer scaffolds ($p<0.05$). The amount grew after the first three days and remained a constant value of about 1.2μg for the next four days. Cells present on the scaffolds however lacked the ability to proliferate. The DNA content started at a low amount after initial seeding of the C3H cells and remained at an approximate value of 0.2μg throughout the entire experimental timeframe. During day 3 and 7, there appeared to be a slight increase of cell growth up to 0.4μg of DNA. It was found however that there was no statistical difference between the amount of DNA measured on day 3 compared to day 7 ($p>0.05$).

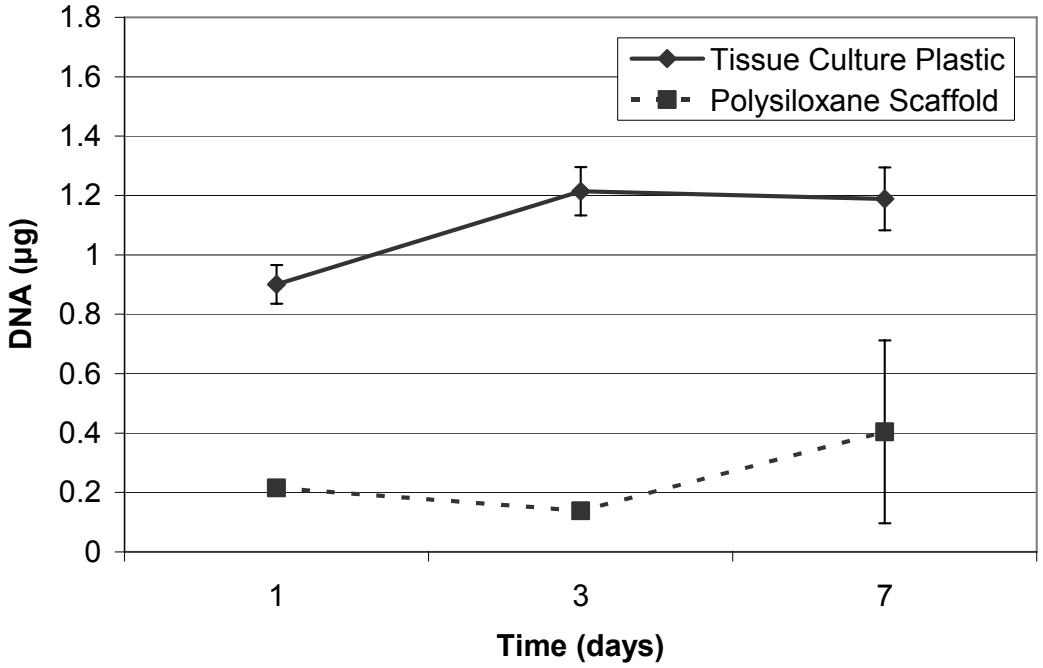

Figure 24. DNA contents from C3H cells cultured on blank scaffolds (n=3) and on tissue culture plastic after periods of 1, 3, and 7 days.

5. Discussion

Due to their effectiveness in specific recognition of biomolecules, molecularly imprinted polymers are being developed for many chemical and medical applications, including solid phase extraction and chromatography, biosensors, and signaling polymers [55]. MIPs also have potential for use in tissue engineering, a discipline that brings together biology and the science of materials. For example, substrates that selectively bind particular proteins in a physiological environment can facilitate desired cell and tissue responses, which are critically dependent on the type and nature of adsorbed biomolecules [34].

5.1. Fabrication of Scaffolds

The process of creating scaffolds for the investigation of molecular imprinting protein is not yet an exact science. Several challenges have been identified concerning imprinting protein into molecularly imprinted polymers, such as problems with the high flexibility of the conformation [56] and complexity of

surface structures inducing poor accessibility of the binding sites, low binding capacity, and large non-specific binding [4]. Solutions to creating efficient scaffolds lie within both the protein that is being imprinted and the material that constitutes the imprint. For instance, Shi et al. investigated imprinting protein using radio frequency glow-discharge plasma deposition to form polymeric thin films around proteins coated with disaccharide molecules with the intent of improving binding efficiency. The disaccharides attached to the polymer film and created cavities that exhibited selective recognition for many template molecules [57].

The properties of a protein, both physical and chemical, make the fabrication process difficult. The conformation of a protein is quite flexible, and while an imprint of the protein is made in one position, it may be difficult for another protein of the same type to perfectly fit that original shape [4]. In addition, the three dimensional configuration of the functional groups within a protein gives rise to a challenging situation for another to rebind with the same orientation when coming in contact with the surface of the imprint. The orientation, for instance, of the peptide imprint might not allow binding of the whole protein because it does not precisely match its conformation (Figure 8). In many cases, the effectiveness of the molecular recognition depend on both the matrix functional monomers and cross-linking monomers [48].

Because of its potential for greater stability, silica was used for the present studies [54]. During polycondensation to form the polysiloxane network, amino groups on the functional monomer aminopropyltriethoxysilane (APS) are able to interact with the template (protein or peptide). The tetraethoxysilane (TEOS) molecules then cross-linked the monomers and locked the template into its position in the silica. The sol-gel processing to fabricate scaffolds was simple, but to make macroporous (foamed) scaffolds, samples were made one at a time, which led to variability between scaffolds, as reflected in some of the results presented. Splattering of the material as it mixes creates a loss of polymer volume and protein that could contribute to more imprints. Also, grinding is done manually, which leads to scaffolds of various shapes, volumes, and surface

areas, and hence inconsistent data markings. One aspect of the grinding step that has not yet been explored is the effect of heat generated from friction. It may be possible that this energy not only disrupts the surface of the polymer but the conformation of the protein imprinted onto the scaffold as well. If this were the case, the release profile of the protein during the maximum loading test may be affected since the damage to the protein via grinding may inhibit fluorescence intensity.

A side experiment conducted in the study was done to test scaffold volume variability and its effects on protein loading capacity. This involved the fabrication of two groups of scaffolds, one with a normal volume of polymerization mix and another with two-thirds the normal volume. The noticeable difference in structure and shape of the partial volume scaffolds after grinding can be explained by how they were made. Unlike the normal scaffolds, the partial volume scaffolds were made in glass vials (plastic vials were used for normal fabrication). The difference in tube material could have an interaction with the polymer itself, leading to an increase in residual mix left on the sides of the cylinder. A smaller bulk polymerization mix volume will have a greater tendency to splash around the tube instead of staying stable while mixing. Another potential cause for the difference in scaffold structure between the two was in the grinding step. Grinding the scaffolds serves as a means to make each a similar shape and to remove the glassy layer that interferes with protein imprinting. The smaller scaffolds are harder to hold, therefore harder to shape and are structurally less stable since less material is present. This creates a larger variability in the physical characteristics of the partial volume scaffolds, which may lead to greater experimental variations in data.

5.2. Protein Maximum Loading Capacity

Maximum loading capacity experiments were useful in that they determined the amount of surface protein or peptide that remained on the scaffolds and therefore the amount of potential imprints available for specific rebinding. Due to the porous nature of the scaffolds, the digested protein was

released from the surface at an exponential rate with a plateau close to 24 hours. Protein or peptide exposed on the outer portion of the scaffold was digested and released quickly, while those within the pores took longer to diffuse outward.

The results for the maximum loading capacity for the lysozyme and lysozyme C peptide imprinted scaffolds are shown in Table 1. A larger mass percentage (about 26%) of lysozyme protein was released from the scaffolds compared to the peptide-imprinted samples. Reasons for the release behavior for each type of scaffold could depend on the size of the molecules as well as interactions between them and the surrounding polymer. More peptide could be embedded in the polymer beyond the reach of the protease so that less is able to release from the surface (due to sol-gel processing). Having such a large molecule digest the small peptide would prove to be difficult since the imprint is so small. The larger, entire protein molecule despite the smaller quantity would be able to expose itself to a higher amount of surface area where it would be vulnerable to protease digestion (Figure 8).

Surprisingly, results showed that for the partial volume polymerization mix experiment, the same amount of lysozyme C peptide was released from both normal and two-thirds volume scaffolds. This suggests that an increase in surface density, or a higher ratio of mass per scaffold volume (volume density), will not change the amount of released peptide because of a saturation in the amount that can occupy space within the polymer. One would expect that the increase in density would allow more peptide molecules to be exposed on the surface since more are available per unit volume. However, this was not the case. Much of the peptide added in the polymerization mix was embedded into the bulk of the polymer and not surface accessible for digestion and creating imprints. This capping or saturation of peptide in the scaffolds may be explained by the space the molecules occupy around the pores. Vigorous mixing of the polymerization mix with the vortex device creates many tiny bubbles due to the presence of SDS. Once there is a layer of peptide around the pore, the affinity for another peptide to bind the surface is very small. This prevents all of the peptide from polymerizing with the polymer at the surface, so any extra is

embedded into the bulk solid. As the peptide is digested, only those on the surface are released and quantitatively measured while the large amount of peptide embedded in the bulk is not. This may be the reason why decreasing the volume and increasing the peptide amount does not change the amount released from the surface. In one study, Chipot and Pohorille determined that the behavior of peptides on membrane interfaces depended on hydrophobic effects, intramolecular hydrogen bonding, and interactions with interfacial electrical fields [58]. In other words, the structure of the peptide may be influenced by the chemistry of the membrane that it is exposed to, which might explain the peptide's affinity to certain air-gel surfaces and bulk polymer interfaces, each with their own surface chemistry characteristics [58].

5.3. Protein Preferential Binding

5.3.1. Lysozyme Protein vs. Lysozyme C Peptide Imprinted Scaffolds

The results from the lysozyme-imprinted scaffold experiments showed excellent preferential binding. The template protein bound significantly more to the polymer scaffolds than the competitor on both the individual exposure level (1:0 and 0:1) and in the 1:1 lysozyme to RNase A competitive level. The experiments showed that successful preferential binding can be achieved by using proteins as imprints to rebind the template molecule. The results for the peptide-imprinted scaffolds, however, did not share the same statistical soundness. Bonferroni post test determined that there was a significant difference in the binding of lysozyme compared to RNase A for the 1:0 and 0:1 ratio but not for the competitive 1:1 ratio case. Similarly, for the total percent of bound protein, there was not a statistical difference of preferential binding in any case. In other words, the data suggest that using peptides as imprints to preferentially bind the protein may not be as effective as when imprinting the entire molecule.

The extremely large variability found in Figure 20 and Figure 21 challenges the efficiency of peptide imprinted polymers to allow for preferential protein binding. The trends, however, in each of these graphs are very similar to

that of the lysozyme protein imprinting data, as are the average values for each ratio. This suggests that preferential binding could still be accomplished if the variability was reduced. Note how in Table 5 that the amount of protein that binds to the blank scaffolds is relatively similar to the amount that binds the imprinted scaffolds. Subtracting the blank values would therefore decrease the amount of peptide that binds due to the influence of imprinting, but keep the standard deviations approximately the same.

Another source of error is believed to come from variability in the structure of the scaffolds. When the scaffolds are fabricated, grinding of the scaffolds is done on an individual basis. This creates scaffolds of different dimensions and shapes, ultimately affecting the internal structure of the molecular imprints and accessibility of the binding sites. The variation in the scaffold structure produces different characteristics for each scaffold, and therefore induces a wide variation in the results. These variations are responsible for the statistical insignificance determined in the ANOVA and Bonferroni post tests for peptide imprinted scaffolds.

In the present study, template release and binding occurred through a non-covalent mechanism, which utilized hydrogen bonding, Van der Waals forces, ionic bonds and hydrophobic interactions with protein recognition cavities. The protein was imprinted into an inorganic polymer consisting of a siloxane bonded network. Solutions to finding more efficient protein imprinting have been explored by altering the template molecule and the structure of the polymer in which it's imprinted. For example, in a study done by Shiomi et al., a new molecular imprinting technique using covalently immobilized hemoglobin (Hb) recognition cavities on silica was explored [56]. Instead of TEOS and APS as polymer components, organic 3-aminopropyltrimethoxysilane (APTMS), and trimethoxypropylsilane (TMPS) were used. Polymerization took place on a surface with covalently immobilized hemoglobin using imine bonds. Imprints were then created by the release of the protein via oxalic acid, instead of the protease used in the current study to release the lysozyme and BMP-2. The hemoglobin-imprinted silica using covalently immobilized Hb as a template

proved to be better than using silica with free Hb regarding selective re-adsorption as compared with other non-template proteins [56].

The amount of protein preferentially bound to the scaffolds was compared to ascertain whether or not imprinting the polymers with lysozyme C peptide was just as effective as imprinting with lysozyme protein. It was hypothesized that specific binding of the protein could be achieved by imprinting only a small peptide section of the molecule, similar to binding an antigen to an antibody utilizing only the epitope region. The t tests showed that compared to each other, the peptide imprinted scaffolds did not significantly bind a different amount of lysozyme than the protein imprinted scaffolds. Amongst themselves, trends of preferential binding could be seen, but between the two types of scaffolds, no difference was observed.

The power analysis determined that for a significant difference in binding of lysozyme to both types of imprinted scaffolds to be seen under competition (1:1 ratio), a sample size of 52 would be necessary. In other words, using the same fabrication methods, there is an 80% chance of finding a significant difference with 52 scaffolds. This number is extremely low compared to the values determined for the noncompetitive cases and the binding of RNase A under competition. This observation suggests that binding of the template protein under a competitive condition was more distinguished than in the solo case. Lysozyme was able to more consistently bind the imprint when it was under competition with RNase A. This interesting property may be explicable by exploring the difference in behavior of the protein and peptide imprinted scaffolds. When a biomaterial enters the body, a series of proteins adsorb and release from the surface in sequential order based on their binding affinity towards the material [26]. Perhaps the binding behavior in this case may be understood in this new light. Under competition, binding of the RNase A may first take place. Since the template has a larger affinity for the imprint, the competitor is released and replaced by lysozyme. The kinetics involved in this phenomenon may be unique for each type of imprinted scaffolds, making the two binding behaviors more distinguishable. This would create the possibility of both protein

and peptide imprinted scaffolds having a significantly different amount of template molecule bind the surface.

Successful rebinding of peptides using the epitope approach was seen, however, in a study performed by Rachkova and Minourab involving oxytocin-related peptides in aqueous media [59]. Instead of using inorganic polymer components for scaffolds, methacrylic acid (MAA) was used as a functional monomer and ethylene glycol dimethylacrylate (EGDMA) was used as a cross-linker. The lysozyme C peptide was chosen for the present study because of its position on the lysozyme protein for surface recognition. Rachkova and Minourab utilized the hormone oxytocin because its tail end C-terminus structure could be recognized with the MAA functional monomers in the imprint created by the tetrapeptide template. Success in the experiment may have come from the simplicity of peptide-surface interaction and small size of the binding molecules. For instance, the peptides used in Rachkova and Minourab's study were 4-10 amino acids in length, compared to lysozyme C peptide which was 18 amino acids in length. In the present study, a large protein was used to test if a small peptide from its surface was able to bind, which is dissimilar to Rachkova and Minourab's study where a small section of a peptide bound to imprints made from another peptide with a slightly smaller length.

5.3.2. BMP-2 Imprinted Scaffolds

BMP-2 was chosen as a template molecule for molecular imprinting in polysiloxane scaffolds because of its use as an important growth factor in the bone healing process [30]. Preferential binding of BMP-2 on imprinted polymers has the potential to be quite useful in applications where biomaterial compatibility and bone tissue growth are of importance. It is hypothesized that when BMP-2 imprinted polymers are implanted in a critical size bone defect, BMP-2 molecules released due to the wound healing response will have the greatest affinity for the imprinted crevices and adsorb on the surface. This control of preferential binding could facilitate and expedite the cellular activity responsible for osteogenesis.

The results from the BMP-2 preferential binding tests showed more specific binding on scaffolds under noncompetitive conditions than for those with a protein ratio of 1:1 (BMP-2 to trypsin). For both amount and percentage bound to the scaffolds, there was no statistical difference between the two types of protein that bound the surface. While a very slight difference in the percentage bound can be seen in the results of Table 7, the standard deviation nullifies any conclusion of BMP-2 binding more than trypsin. A large standard deviation is the result of a variation in scaffold properties. Each scaffold is individually prepared, starting from the addition of protein during polymerization and ending with the grinding to make the shape as consistent as possible to the standard dimensions. Because each scaffold will vary slightly in such details as initial protein amount, number of imprints, amount of available binding sites exposed to the surface, surface area, pore size, and porosity, the number of template as well as competitor molecules that bind will also vary. This problem might be fixed using methods that eliminate individual manual processing. New technologies are being explored in rapid prototyping such as solid free-form fabrication that may one day address this issue [60]. Another concern may have been the actual amount of protein added to the polymerization mix. In previous experiments [54], much more than 30μg of protein was added to the polymerization mix. Significant preferential binding results using 100, 1000 and 3000μg were accomplished while using lysozyme. The difficulty with using BMP-2 as a potential protein for molecular imprinting is that using amounts of 3000μg for multiple experiments would be unfeasible due to price and the exorbitant amount used.

The amount of protein that bound the scaffold solely due to imprinting was found by subtracting the percent that bound to the non-imprinted scaffolds. This gives negative values for trypsin binding amounts. This means that the blank scaffolds bound higher quantities of trypsin than the imprinted scaffolds. The negative value for trypsin binding to the scaffolds with a protein ratio of 0:1 (template to competitor) is an interesting observation, as it suggests that the BMP-2 imprinted scaffolds may have a repelling effect on proteins that do not fit

into the special imprints. In other words, the surface of the scaffolds is shielded from non-specific binding. This observation is only seen with the trypsin competitor and not seen with binding of the RNase A. This might suggest, as speculated, that the chemistry of the molecular imprint is not allowing for non-specific binding of the trypsin to the polymer surface, similar to how the surface chemistry of biomaterial surfaces minimize non-specific binding of adhesion proteins upon contact with blood [26, 61]. Further studies would need to take place to assess whether this feature would be beneficial in tissue-material interactions. Whether this phenomenon is desirable or not would depend on the results of such studies and its application as a biomaterial.

Studies of BMP-2 adhesion on porous scaffolds for bone induction are not uncommon, and a limited release of the protein from the scaffolds is also observed. For instance, BMP-2 released from porous calcium phosphate (Ca-P) cement was studied by Ruhé et al. to evaluate the scaffolds' osteoinductive properties in rabbit cranial defects [62]. Unlike using silica polymers fabricated by the sol-gel process, the group utilized calcium phosphate cement with a carbon dioxide induction technique to create the porous scaffold. An amount of 10μg of BMP-2 (recombinant human or rhBMP-2) was adsorbed on the surface of the scaffolds by pipette. Release profiles were carried out in an additional study to determine whether the bone formation was induced by a relatively high concentration of growth factor in the surrounding tissues. The study revealed that only a limited release of the loaded rhBMP-2 (9.7 ± 0.9 %) had occurred cumulatively over a 28 day period. These results along with the results of the present study suggest that the absorption properties of BMP-2 may still not be fully understood, and further study of the protein-material interface for BMP-2 is required for more efficient specific binding.

5.4. Cytocompatibility

The initial *in vitro* testing of the molecularly imprinted polysiloxane scaffolds for bone biomaterial applications involved ensuring that osteogenic cells had the ability to remain viable on the polymer surface under controlled

environments. As a control to compare the polymer's performance, cells were grown on tissue culture plastic on the bottom of the culture plates. As with most tissue or cell culture plastic, cells are highly compatible with the surface due to its hydrophilic nature and good physical properties. In this case cells would be able to adhere and spread on the surface very quickly, and in the few days following become a confluent multi-layered sheet. The results of the cytocompatibility test are evidence that this is true (Figure 24). After one day of incubation on the tissue culture plastic, a high amount of DNA content was recorded. By day 3, the amount of cells on the surface was beginning to reach its capacity. This can be assumed from the fact that by day 7 the amount of DNA content has not changed. This behavior of cellular growth is compared to the pattern for growth on the polysiloxane scaffolds for effective cell viability.

C3H growth on the polysiloxane scaffolds was measured at very small values. While it was apparent that cells did exist on the surface of the scaffolds, substantial growth during the 1 week incubation period was not observed. The DNA content decreased slightly during the 1-3 day interval and then increased up to day 7, however statistical analysis showed that there was no significant difference in growth at that time. A few reasons could have accounted for the growth rate behavior of the cells on the polymer scaffolds. The most apparent cause for such a large difference in cell growth existed between the tissue culture plastic and porous polymer was the different surface chemistry. Tissue culture plastic is made of polystyrene that is oxidized to increase hydrophilicity, which results in abundant protein adsorption that enables cells to easily attach and spread out. The surface of the polysiloxane on the other hand was mostly non-polar due to the large influence of the stable TEOS cross-linker chemical, and may have been responsible for low cell attachment.

Another possible cause for low cell adhesion could be that a very small number of cells were actually present on the scaffold surface once incubation began. The cells were seeded on the polymer scaffolds in a very small volume of medium to achieve a high surface density of cells. The scaffolds were then incubated for 2 hours to allow for the cells to infiltrate the pores and attach to the

surface. If the cells are not all properly attached, addition of the 5mL of medium will cause them to lift off of the surface and into the surrounding solution. Not all of the cells are able to fit on the top surface before the 2 hour incubation period, so even less therefore are able to grow and are measured after the 1 week time span. The reason for this event may be due to the actual physical properties of the scaffolds. In a study performed by Borden et al., osteoblasts cells were seeded on poly(lactide-co-glicolide) (PLAGA) sintered scaffolds. The group was able to fabricate an "optimal scaffold" with a median pore size of 210μm and a porosity of 35% from heated microspheres [63]. They reported that after 7 and 16 days, SEM results indicated that the cells had attached and proliferated through the microsphere pore system. The polysiloxane scaffolds used for cell seeding in the present study had similar a porosity (43%) but a very small average pore size diameter (approximately 6.2μm). Such a small pore size could be responsible for low cell infiltration during the 2 hour seed incubation period and therefore lead to cells washing off the surface of the scaffold during medium addition. Cells that did wash off into the wells were observable under the light microscope, and throughout the entire incubation period appeared to be quite healthy. This indicates that the reason for low DNA content might not be due to malevolent factors such as the release ethanol from the scaffolds or any changes in pH.

Once it can be shown that cells were able to survive on the surface of the scaffolds, the next phase would be determining if cellular activity could be influenced by the preferential binding of BMP-2 on the imprinted scaffolds. As an *in vitro* experiment, the system under control must simulate the cells' natural environment as closely as possible until there is enough evidence that the material can perform well *in vivo*. For molecularly imprinted polymers in the use of tissue engineered bone scaffolds, that possibility is coming steadily closer.

6. Conclusions

The potential for protein imprinted polymers has been shown, as well as trends of the same preferential binding with the imprinting of peptides and biologically relevant proteins. Fabrication of the scaffolds was accomplished using a sol-gel processing technique, which entrapped protein and water in the polymer matrix via siloxane bonds. The scaffolds were characterized by the amount and number of protein molecules that released from the porous surface after proteolytic digestion with a protease enzyme mixture. The unloading capacity on all scaffolds ranged from about 40% to 80%, which approximated the number of available binding sites on the scaffolds. This value approximated the amount of protein that was re-exposed to test for preferential binding. Lysozyme, a protein not important for bone formation, preferentially bound about 1.71 ± 0.01μg. Peptide imprinted scaffolds preferentially bound about 0.55 ± 2.95μg of the whole protein. BMP-2 imprinted scaffolds preferentially rebound 0.075 ± 0.52μg. All were under competition of a protein that was similar in molecular weight, but different in chemistry. Errors in the data produced large standard deviations, most of which were present because of large non-specific binding of the competitors on the imprinted scaffolds, protein conformation stability, fabrication and protein imprinting orientation issues. While it is apparent that perfecting the art is still far away, there is evidence that molecularly imprinted polymers have the potential to be key players in the realm of protein and cell interactions for tissue engineering and biomaterial integration. For further *in vitro* study, the viability and activity of cells on BMP-2 imprinted scaffolds, (both empty imprints and imprints with preferentially bound protein) for the control of cellular behavior, should be performed.

References

1. Katti, K. S., *Biomaterials in total joint replacement.* Colloids and Surfaces B: Biointerfaces, 2004. 39(3): p. 133-142.
2. Langer, R. and J. P. Vacanti, *Tissue engineering.* Science, 1993. 260(5110): p. 920-926.
3. Stock, U. A. and J. P. Vacanti, *Tissue engineering: Current state and prospects.* Annual Review of Medicine, 2001. 52: p. 443-451.
4. Bossi, A., F. Bonini, A. P. F. Turner and S. A. Piletsky, *Molecularly imprinted polymers for the recognition of proteins: The state of the art.* Biosensors and Bioelectronics, 2007. 22(6): p. 1131-1137.
5. Rachkov, A. and N. Minoura, *Towards molecularly imprinted polymers selective to peptides and proteins. The epitope approach.* Biochimica et Biophysica Acta (BBA) - Protein Structure and Molecular Enzymology, 2001. 1544(1-2): p. 255-266.
6. Silvestri, D., N. Barbani, C. Cristallini, P. Giusti and G. Ciardelli, *Molecularly imprinted membranes for an improved recognition of biomolecules in aqueous medium.* Journal of Membrane Science, 2006. 282(1-2): p. 284-295.
7. Odabasi, M., R. Say and A. Denizli, *Molecular imprinted particles for lysozyme purification.* Materials Science and Engineering: C, 2007. 27(1): p. 90-99.
8. Weinstein, L. P. and D. P. Hanel, *Metacarpal fractures.* Journal of the American Society for Surgery of the Hand, 2002. 2(4): p. 168-180.
9. Kregor, P. J., J. Stannard, M. Zlowodzki, P. A. Cole and J. Alonso, *Distal femoral fracture fixation utilizing the Less Invasive Stabilization System (L.I.S.S.): The technique and early results.* Injury, 2001. 32(Supplement 3): p. 32-47.
10. Torta, G. J. and S. R. Grabowski, *Principles of Anatomy and Physiology*. Tenth ed. 2003, New Jersey: John Wiley & Sons, Inc.
11. Browner, B. D., F. G. Alberta and D. J. Mastella, *A new era in orthopedic trauma care.* Surgical Clinics of North America, 1999. 79(6): p. 1431-1448.
12. McKinley, T., *Principles of Fracture Healing.* Surgery (Oxford), 2003. 21(9): p. 209-212.
13. Kesemenli, C., M. Subasi, S. Necmioglu and A. Kapukaya, *Treatment of multifragmentary fractures of the femur by indirect reduction (biological) and plate fixation.* Injury, 2002. 33(8): p. 691-699.
14. Sledge Iii, J. B., *Management of Femoral Neck Stress Fractures.* Operative Techniques in Sports Medicine, 2006. 14(4): p. 265-269.
15. Arnold, J. S., *A simplified model of wound healing III-the critical size defect in three dimensions.* Mathematical and Computer Modelling, 2001. 34: p. 385-392.
16. Lewis, P. L., N. T. Brewster and S. E. Graves, *The pathogenesis of bone loss following total knee arthorplasty.* Orthopedic Clinics of North America, 1998. 29(2): p. 187-197.
17. Hartsfield, J. J. K., W. F. Hohlt and W. E. Roberts, *Orthodontic treatment and orthognathic surgery for patients with osteogenesis imperfecta.* Seminars in Orthodontics, 2006. 12(4): p. 254-271.
18. Rose, F. R. A. J. and R. O. C. Oreffo, *Bone tissue engineering: hope vs hype.* Biochemical and Biophysical Research Communications, 2002. 292(1): p. 1-7.

19. Burg, K. J. L., S. Porter and J. F. Kellam, *Biomaterial developments for bone tissue engineering.* Biomaterials, 2000. 21(23): p. 2347-2359.
20. Yoshikawa, T., *Bone reconstruction by cultured bone graft.* Materials Science and Engineering: C, 2000. 13(1-2): p. 29-37.
21. Borden, M., M. Attawia, Y. Khan and C. T. Laurencin, *Tissue engineered microsphere-based matrices for bone repair: design and evaluation.* Biomaterials, 2002. 23(2): p. 551-559.
22. Thull, R., *Physicochemical principles of tissue material interactions.* Biomolecular Engineering, 2002. 19(2-6): p. 43-50.
23. Puleo, D. A. and A. Nanci, *Understanding and controlling the bone-implant interface.* Biomaterials, 1999. 20(23-24): p. 2311-2321.
24. Aukhil, I., *Biology of wound healing.* Periodontoloty 2000, 2000. 22: p. 44-50.
25. Werner, S. and R. Grose, *Regulation of wound healing by growth factors and cytokines.* Physiol. Rev., 2003. 83(3): p. 835-870.
26. Ratner, B. D., A. S. Hoffman, F. J. Schoen and J. E. Lemon, *Biomaterials Science*. Second ed. 2004, Amsterdam: Elsevier Academic Press.
27. Heppenstall, R. B., C. W. Goodwin and C. T. Brighton, *Fracture healing in the presence of chronic hypoxia.* Journal of Bone and Joint Surgery 1976. 58(8): p. 1153-1156.
28. Vaananen, H. K., Y.-k. Liu, P. Lehenkari and T. Uemara, *How do osteoclasts resorb bone?* Materials Science and Engineering: C, 1998. 6(4): p. 205-209.
29. Groeneveld, E. H. and E. H. Burger, *Bone morphogenetic proteins in human bone regeneration.* European Journal of Endocrinology, 2000. 142(1): p. 9-21.
30. Lee, M. B., *Bone morphogenetic proteins: background and implications for oral reconstruction. A review.* Journal of Clinical Periodontology, 1997. 24(6): p. 355-365.
31. Shin, H., S. Jo and A. G. Mikos, *Biomimetic materials for tissue engineering.* Biomaterials, 2003. 24(24): p. 4353-4364.
32. Kofron, M. D. and C. T. Laurencin, *Bone tissue engineering by gene delivery.* Advanced Drug Delivery Reviews, 2006. 58(4): p. 555-576.
33. Schwartz, Z., K. Kieswetter, D. D. Dean and B. D. Boyan, *Underlying mechanisms at the bone-surface interface during regeneration.* Journal of Periodontal Research, 1997. 32(1): p. 166-171.
34. Sawyer, A. A., K. M. Hennessy and S. L. Bellis, *The effect of adsorbed serum proteins, RGD and proteoglycan-binding peptides on the adhesion of mesenchymal stem cells to hydroxyapatite.* Biomaterials, 2007. 28(3): p. 383-392.
35. Kim, B.-S. and D. J. Mooney, *Development of biocompatible synthetic extracellular matrices for tissue engineering.* Trends in Biotechnology, 1998. 16(5): p. 224-230.
36. Baldwin, S. P. and W. Mark Saltzman, *Materials for protein delivery in tissue engineering.* Advanced Drug Delivery Reviews, 1998. 33(1-2): p. 71-86.
37. McMurry, *Organic Chemistry*. 6 ed. 2004, Austrailia: Thomson.
38. Chesko, J., J. Kazzaz, M. Ugozzoli, D. T. O'Hagan and M. Singh, *An investigation of the factors controlling the adsorption of protein antigens to anionic PLG microparticles.* Journal of Pharmaceutical Sciences, 2005. 94(11): p. 2510-2519.
39. Anselme, K., *Osteoblast adhesion on biomaterials.* Biomaterials, 2000. 21(7): p. 667-681.

40. Wozney, J. M. and H. J. Seeherman, *Protein-based tissue engineering in bone and cartilage repair.* Current Opinion in Biotechnology, 2004. 15(5): p. 392-398.
41. Derner, R. and A. C. Anderson, *The bone morphogenic protein.* Clinics in Podiatric Medicine and Surgery, 2005. 22(4): p. 607-618.
42. Keller, S., J. Nickel, J.-L. Zhang, W. Sebald and T. D. Mueller, *Molecular recognition of BMP-2 and BMP receptor IA.* Nature Structural & Molecular Biology, 2004. 11(5): p. 481-488.
43. Nilsson, J., P. Spegel and S. Nilsson, *Molecularly imprinted polymer formats for capillary electrochromatography.* Journal of Chromatography B, 2004. 804(1): p. 3-12.
44. Sellergren, B., *Noncovalent molecular imprinting: antibody-like molecular recognition in polymeric network materials.* TrAC Trends in Analytical Chemistry, 1997. 16(6): p. 310-320.
45. Wei, S., M. Jakusch and B. Mizaikoff, *Capturing molecules with templated materials: Analysis and rational design of molecularly imprinted polymers.* Analytica Chimica Acta, 2006. 578(1): p. 50-58.
46. Sellergren, B. and C. J. Allender, *Molecularly imprinted polymers: A bridge to advanced drug delivery.* Advanced Drug Delivery Reviews, 2005. 57(12): p. 1733-1741.
47. Byrne, M. E., K. Park and N. A. Peppas, *Molecular imprinting within hydrogels.* Advanced Drug Delivery Reviews, 2002. 54(1): p. 149-161.
48. Lin, H.-Y., C.-Y. Hsu, J. L. Thomas, S.-E. Wang, H.-C. Chen and T.-C. Chou, *The microcontact imprinting of proteins: The effect of cross-linking monomers for lysozyme, ribonuclease A and myoglobin.* Biosensors and Bioelectronics, 2006. 22(4): p. 534-543.
49. Spivak, D. A., *Optimization, evaluation, and characterization of molecularly imprinted polymers.* Advanced Drug Delivery Reviews, 2005. 57(12): p. 1779-1794.
50. Venton, D. L. and E. Gudipati, *Influence of protein on polysiloxane polymer formation: evidence for induction of complementary protein-polymer interactions.* Biochimica et Biophysica Acta (BBA) - Protein Structure and Molecular Enzymology, 1995. 1250(2): p. 126-136.
51. Laughlin, J. B., J. L. Sarquis, V. M. Jones and J. A. Cox, *Using sol-gel chemistry to synthesize a material with properties suited for chemical sensing: Development and implementation of a materials science experiment for the undergraduate curriculum* Journal of Chemical Education, 2000. 77(1): p. 77-79.
52. Brinker, C. J., R. Sehgal, S. L. Hietala, R. Deshpande, D. M. Smith, D. Loy and C. S. Ashley, *Sol-gel strategies for controlled porosity inorganic materials.* Journal of Membrane Science, 1994. 94(1): p. 85-102.
53. El-Nahhal, I. M. and N. M. El-Ashgar, *A review on polysiloxane-immobilized ligand systems: Synthesis, characterization and applications.* Journal of Organometallic Chemistry, 2007. 692(14): p. 2861-2886.
54. Lee, K., R. R. Itharaju and D. A. Puleo, *Protein-imprinted polysiloxane scaffolds.* Acta Biomaterialia. In Press, Corrected Proof.
55. Komiyama, M., T. Takeuchi, T. Mukawa and H. Asanuma, *Molecular imprinting: From fundamentals to applications*. 2003: Wiley-VCH. 159.
56. Shiomi, T., M. Matsui, F. Mizukami and K. Sakaguchi, *A method for the molecular imprinting of hemoglobin on silica surfaces using silanes.* Biomaterials, 2005. 26(27): p. 5564-5571.

57. Shi, H., W.-B. Tsai, M. D. Garrison, S. Ferrari and B. D. Ratner, *Template-imprinted nanostructured surfaces for protein recognition.* Nature, 1999. 398(6728): p. 593-597.
58. Chipot, C. and A. Pohorille, *Structure and dynamics of small peptides at aqueous interfaces a multi-nanosecond molecular dynamics study.* Journal of Molecular Structure: THEOCHEM, 1997. 398-399: p. 529-535.
59. Rachkov, A. and N. Minoura, *Recognition of oxytocin and oxytocin-related peptides in aqueous media using a molecularly imprinted polymer synthesized by the epitope approach.* Journal of Chromatography A, 2000. 889(1-2): p. 111-118.
60. Leong, K. F., C. M. Cheah and C. K. Chua, *Solid freeform fabrication of three-dimensional scaffolds for engineering replacement tissues and organs.* Biomaterials, 2003. 24(13): p. 2363-2378.
61. Sun, S., Y. Yue, X. Huang and D. Meng, *Protein adsorption on blood-contact membranes.* Journal of Membrane Science, 2003. 222(1-2): p. 3-18.
62. Ruhe, P. Q., H. C. Kroese-Deutman, J. G. C. Wolke, P. H. M. Spauwen and J. A. Jansen, *Bone inductive properties of rhBMP-2 loaded porous calcium phosphate cement implants in cranial defects in rabbits.* Biomaterials, 2004. 25(11): p. 2123-2132.
63. Borden, M., S. F. El-Amin, M. Attawia and C. T. Laurencin, *Structural and human cellular assessment of a novel microsphere-based tissue engineered scaffold for bone repair.* Biomaterials, 2003. 24(4): p. 597-609.

Vita

Michael Edward Brown was born on May 2, 1983 in Murfreesboro, Tennessee, USA. He received his Bachelor of Science degree in Agriculture and Biosystems Engineering at the University of Arizona in Tucson, Arizona in May of 2005. While attending school, he worked at the Genomic Analysis and Technology Core, Inc., a human genetics laboratory from June of 2004 to May of 2005. He began his Masters program at the Center for Biomedical Engineering at the University of Kentucky in Lexington, Kentucky in August of 2005. Michael also attended the Society for Biomaterials Annual meeting in Pittsburgh, Pennsylvania in April of 2006 and the CALBIO 2007 Annual meeting in San Diego, California in March 2007, and later presented a poster at the Society for Biomaterials Annual meeting in April of 2007.